Variation in Crossover Frequencies Perturb Crossover Assurance Without Affecting Meiotic Chromosome Segregation in *Saccharomyces cerevisiae*

Gurukripa N. Krishnaprasad,* Mayakonda T. Anand,* Gen Lin,† Manu M. Tekkedil,† Lars M. Steinmetz,†,‡,§ and Koodali T. Nishant*,[1]

*School of Biology, Indian Institute of Science Education and Research, Thiruvananthapuram, Trivandrum 695016, India, †European Molecular Biology Laboratory, Genome Biology Unit, 69117, Heidelberg, Germany, ‡Department of Genetics, Stanford University, Stanford, California 94305, §Stanford Genome Technology Center, Palo Alto, California 94304

ABSTRACT The segregation of homologous chromosomes during the Meiosis I division requires an obligate crossover per homolog pair (crossover assurance). In *Saccharomyces cerevisiae* and mammals, Msh4 and Msh5 proteins stabilize Holliday junctions and its progenitors to facilitate crossing over. *S. cerevisiae msh4/5* hypomorphs that reduce crossover levels up to twofold at specific loci on chromosomes VII, VIII, and XV without affecting homolog segregation were identified recently. We use the *msh4–R676W* hypomorph to ask if the obligate crossover is insulated from variation in crossover frequencies, using a *S. cerevisiae* S288c/YJM789 hybrid to map recombination genome-wide. The *msh4–R676W* hypomorph made on average 64 crossovers per meiosis compared to 94 made in wild type and 49 in the *msh4Δ* mutant confirming the defect seen at individual loci on a genome-wide scale. Crossover reductions in *msh4–R676W* and *msh4Δ* were significant across chromosomes regardless of size, unlike previous observations made at specific loci. The *msh4–R676W* hypomorph showed reduced crossover interference. Although crossover reduction in *msh4–R676W* is modest, 42% of the four viable spore tetrads showed nonexchange chromosomes. These results, along with modeling of crossover distribution, suggest the significant reduction in crossovers across chromosomes and the loss of interference compromises the obligate crossover in the *msh4* hypomorph. The high spore viability of the *msh4* hypomorph is maintained by efficient segregation of the natural nonexchange chromosomes. Our results suggest that variation in crossover frequencies can compromise the obligate crossover and also support a mechanistic role for interference in obligate crossover formation.

KEYWORDS crossover assurance; obligate crossover; genome-wide recombination map; whole-genome sequencing; nonexchange chromosomes

SEXUALLY reproducing organisms undergo meiosis to produce haploid gametes from diploid progenitor cells (Roeder 1997; Zickler and Kleckner 1999). This reduction in ploidy is achieved through the segregation of homologous chromosomes at the first meiotic division (MI). Accurate homolog segregation is facilitated by crossovers that establish physical connections between homolog pairs and provide tension necessary for generation of the bipolar spindle (Petronczki *et al.* 2003). Meiotic crossing over is highly regulated to ensure at least one crossover per homolog pair (crossover assurance) despite limited number of crossovers per meiosis (Berchowitz and Copenhaver 2010; Rosu *et al.* 2011).

Although crossovers are thought to be essential for accurate meiotic chromosome segregation, population genetic studies in humans suggest that there is considerable variation in crossover frequencies between populations, sexes, and individuals (Cheung *et al.* 2007; Chowdhury *et al.* 2009; Fledel-Alon *et al.* 2009; Kong *et al.* 2010; Kong *et al.* 2014). Analysis of meiotic crossovers in single sperm cells using whole-genome sequencing reinforces the fact that within individuals, crossover numbers per meiosis vary widely (Lu *et al.*

doi: 10.1534/genetics.114.172320
Manuscript received November 1, 2014; accepted for publication November 24, 2014; published Early Online December 2, 2014.
Available freely online through the author-supported open access option.
Supporting information is available online at http://www.genetics.org/lookup/suppl/doi:10.1534/genetics.114.172320/-/DC1.
Sequence data from this article have been deposited with the National Centre for Biotechnology Information Sequence Read Archive under accession no. SRP041856.
Processed data and custom R scripts are available from http://figshare.com (http://dx.doi.org/10.6084/m9.figshare.1192705).
[1]Corresponding author: School of Biology, Indian Institute of Science Education and Research Thiruvananthapuram, CET Campus, Trivandrum 695016, India.
E-mail: nishantkt@iisertvm.ac.in

2012). The average number of crossovers per sperm was observed to be 26, but with a large variation from 17 to 35 crossovers per sperm (Lu *et al.* 2012). Although a lower frequency of crossovers increases the chances of aneuploidy in sperm, studies in *Saccharomyces cerevisiae*, *Drosophila*, and humans have shown that nonexchange chromosomes can undergo accurate segregation frequently (Dawson *et al.* 1986; Mann and Davis 1986; Guacci and Kaback 1991; Dernburg *et al.* 1996; Karpen *et al.* 1996; Kemp *et al.* 2004; Cheslock *et al.* 2005; Fledel-Alon *et al.* 2009; Gladstone *et al.* 2009; Newnham *et al.* 2010). Identification of genetic variants associated with such variation in crossover frequencies is of considerable interest.

Meiotic crossovers are initiated by the programmed introduction of DNA double-strand breaks (DSBs) (Keeney *et al.* 1997). Repair of meiotic DSBs results in the formation of crossover as well as noncrossover products through distinct pathways (Allers and Lichten 2001; Hunter and Kleckner 2001). In *S. cerevisiae* and mammals, a majority of the crossovers are formed through a pathway mediated by the MutS mismatch repair homologs Msh4, Msh5, and MutL mismatch repair homologs Mlh1, Mlh3 (Ross-Macdonald and Roeder 1994; Hollingsworth *et al.* 1995; Baker *et al.* 1996; Barlow and Hulten 1998; De Vries *et al.* 1999; Edelmann *et al.* 1999; Woods *et al.* 1999; Kneitz *et al.* 2000; Novak *et al.* 2001; Lipkin *et al.* 2002; Santucci-Darmanin *et al.* 2002; Argueso *et al.* 2004; Guillon *et al.* 2005; Kolas *et al.* 2005; Lynn *et al.* 2007; Cole *et al.* 2012). The Msh4/5 proteins are part of an ensemble of proteins called the ZMM complex that stabilizes single end invasion intermediates generated during invasion of an intact homolog by a resected DSB end (Chua and Roeder 1998; Agarwal and Roeder 2000; Borner *et al.* 2004; Tsubouchi *et al.* 2006; Shinohara *et al.* 2008). The Msh4/5 complex also binds and stabilizes double Holliday junctions and promotes their resolution into crossover products in association with other repair factors that include Mlh1/3, Exo1, and Sgs1 (Borner *et al.* 2004; Snowden *et al.* 2004; Nishant *et al.* 2008; Snowden *et al.* 2008; Zakharyevich *et al.* 2010; De Muyt *et al.* 2012; Zakharyevich *et al.* 2012).

Recent human studies have implicated polymorphisms in *ZMM* genes such as *RNF212* (putative *S. cerevisiae ZIP3* ortholog) and *MSH4* with genome-wide crossover frequency variation (Kong *et al.* 2014). Similar observations have been made in *S. cerevisiae*, where a series of *msh4/5* hypomorphic alleles that showed up to twofold reduction in crossovers at specific loci on chromosomes VII, VIII, and XV with high spore viability were identified (Nishant *et al.* 2010). The high spore viability observed in *S. cerevisiae msh4/5* hypomorphs and in other mutants like *mlh3Δ mms4Δ* (Brown *et al.* 2013) provide further evidence that a reduction in crossovers is not directly correlated with nondisjunction. In this study we use the *S. cerevisiae msh4–R676W* hypomorph as a tool to study how variation in crossover frequencies is buffered by the cell to ensure chromosome segregation. The *msh4–R676W* hypomorph is predicted to be defective in ATP hydrolysis by the Msh4/5 complex (Kijas *et al.* 2003; Nishant *et al.* 2010; Rakshambikai *et al.* 2013). *S. cerevisiae*, *msh4*Δ, and *msh5*Δ mutants have ~2.5-fold reduction in crossing over and ~60% reduction in meiotic viability, and nonexchange chromosomes are observed in the viable spores (Ross-Macdonald and Roeder 1994; Hollingsworth *et al.* 1995; Novak *et al.* 2001; Argueso *et al.* 2004; Chen *et al.* 2008; Oke *et al.* 2014). Comparison of spore viability and genetic map distances for wild type (97%, 96 cM), *msh4–R676W* (90%, 56 cM), and *msh4Δ* (36%, 39 cM) showed that the *msh4* hypomorph has high spore viability despite up to a twofold decrease in crossing over on specific genetic intervals on chromosome XV (Argueso *et al.* 2004; Nishant *et al.* 2010). Two mutually exclusive possibilities can explain this phenomenon. Either *msh4/5* hypomorphs continue to ensure one crossover per homolog pair (crossover assurance) or they segregate nonexchange chromosomes efficiently. To distinguish between these two mechanisms, we sought to examine genome-wide crossover distribution in the *msh4–R676W* hypomorph.

In whole-genome studies, segregation of single nucleotide polymorphisms (SNPs) in crosses of yeast strains are used to track recombination events (Chen *et al.* 2008; Mancera *et al.* 2008; Qi *et al.* 2009; Anderson *et al.* 2011; Martini *et al.* 2011; Oke *et al.* 2014). We made high-resolution genome-wide recombination maps in the *msh4–R676W* hypomorph using an S288c/YJM789 hybrid strain. The *msh4–R676W* hypomorph showed on average ~30% genome-wide reduction in crossover numbers and reduced interference compared to wild type. Although the reduction in crossovers was modest, 42% of the four viable spore meiotic events were observed to have one, or more than one, nonexchange chromosome in the *msh4–R676W* hypomorph. Combined loss of crossovers and interference therefore compromise the obligate crossover in *msh4–R676W*. These results, along with modeling of crossover distribution patterns in wild type and *msh4* mutants, support a mechanistic role for interference in crossover assurance. Despite the large number of meioses with nonexchange chromosomes in the *msh4–R676W* hypomorph, analysis of spore viability patterns suggests efficient segregation of natural nonexchange chromosomes in *S. cerevisiae*.

Materials and Methods

Media and strains

S. cerevisiae S288c and YJM789 yeast strains were grown on either yeast extract–peptone–dextrose (YPD) or synthetic complete medium at 30° (Mortimer and Johnston 1986; Rose *et al.* 1990; McCusker *et al.* 1994). All strains constructed in this study were derived by transformation of S288c and YJM789 *S. cerevisiae* strains with integration plasmids using standard techniques (Gietz *et al.* 1995). When required, the drugs geneticin (Invitrogen), nourseothricin (Werner BioAgents, Germany), and hygromycin (Sigma) were added to the media

at prescribed concentrations (Goldstein and McCusker 1999). Strains are listed in Supporting Information, Table S1. Sporulation medium was prepared as described in Argueso *et al.* (2004).

Tetrad analysis

The haploid strains were patched together on synthetic complete medium and incubated for 4 hr. The resulting diploids were sporulated using standard zero-growth-mating protocol (Argueso *et al.* 2003). After 48 hr in sporulation medium, tetrads were dissected on synthetic complete medium using a Zeiss dissection microscope.

DNA extraction and whole-genome sequencing of meiotic spores

Spore colonies from tetrads were independently cultured overnight at 30° in 4 ml of YPD liquid medium. DNA was extracted from each culture using the PrepEase DNA isolation kit from Affymetrix following the manufacturer's protocol. Genomic DNA fragmentation and library preparation were performed as described previously (Wilkening *et al.* 2013). Briefly, 2 μg of genomic DNA was sheared using a Bandelin Sonorex RX 102 sonicating water bath to obtain DNA fragments of 250–500 bp. End repair, dA-tailing, and ligation were done as per the Illumina library preparation protocol with heat inactivation instead of column/magnetic bead- based cleanups. The multiplexed libraries were amplified and size selected for 350–-400 bp using Invitrogen E-Gel (SizeSelect 2%). The size-selected DNA was sequenced (100PE) on Illumina HiSeq 2000 machines at the EMBL Genomics Core Facilities (GeneCore), Heidelberg, Germany. The raw reads obtained were demultiplexed using the FASTX-toolkit (https://github.com/agordon/fastx_toolkit). Demultiplexed reads were processed for quality control (QC) using the NGS QC Toolkit (Patel and Jain 2012). These QC-filtered high-quality reads were used for further analysis. The sequence data are available from the National Centre for Biotechnology Information Sequence Read Archive under accession no. SRP041856.

Read mapping, genotyping, and annotation of recombination events

We used "ReCombine"—a set of programs developed to analyze the meiotic recombination events from whole-genome sequencing and microarray data from yeast tetrads (Anderson *et al.* 2011). Reads were aligned to both the S288c and YJM789 references using ReadAligner program, which uses native bowtie aligner for alignment (Langmead *et al.* 2009). Since, our read length was ~100 bp and bowtie 1 has limitations in aligning longer reads, each read was broken down into two separate reads of 45 bp each to increase the overall alignment rate. Input parameters for the bowtie aligner in ReadAligner program were also modified to support paired-end alignment. From the alignment, 58,655 SNPs were genotyped. Finally various events such as crossovers, noncrossovers (type 0 gene conversions exhibiting 1:3 or 3:1 segregation of SNP markers), gene conversions not associated with crossovers (type 0, 2, 3, and 4 gene conversions), and crossover-associated gene conversions were detected using the Crossover program (Anderson *et al.* 2011). A 2.5-kb range was set to merge closely placed crossover and noncrossover events. Custom R scripts were written to parse the output files. Plotting was done in R using grammar for graphics 2 (ggplot2) and other base packages. All test statistics were calculated in R (v. 2.15.2, CRAN). The SNP segregation files, data output from the Crossover program, and the custom R scripts are deposited at http://figshare.com (http://dx.doi.org/10.6084/m9.figshare. 1192705).

Detection of copy-number variation

For each alignment of each segregant, read counts were tabulated for consecutive 5000-bp windows using cn.MOPS (Klambauer *et al.* 2012). With the read counts table, segmentation and smoothing was done using default settings in DNAcopy to infer chromosomal copy number (Olshen *et al.* 2004). Allele frequency for each SNP in each segregant was calculated as the number of bases called from the YJM789 allele as a proportion of the total number of bases called.

Interference analysis

Previous studies have suggested that ~250 intercrossover distances (genome-wide crossover data from three tetrads) is sufficient to distinguish between strains with wild-type interference and absence of interference (Chen *et al.* 2008; Anderson *et al.* 2011). We calculated intercrossover distance as the physical distance between consecutive crossovers. These values were converted into genetic distance using the formula: Morgan = $12.07 \times 10^6 \times 2$/mean crossovers. A 1-cM genetic distance was equivalent to 2.56 kb (wild type), 3.75 kb (*msh4–R676W*), and 4.8 kb (*msh4Δ*). Genetic distances between crossovers were modeled as a gamma distribution. The model parameters (α and β) were fitted by maximum-likelihood method. Estimated parameters were tested for goodness of fit by Kolmogorov–Smirnov statistic tests ($P < 0.05$) and Bayesian information criterion (BIC).

Results

High-resolution genome-wide recombination map in the msh4–R676W hypomorph using high-throughput sequencing

We used the *S. cerevisiae* S288c/YJM789 hybrid to generate a high-resolution genome-wide recombination map in the *msh4–R676W* hypomorph. The S288c/YJM789 hybrid has a spore viability of 84%, recombination parameters are similar to the SK1 and S288c strains, and crossovers display interference (Winzeler *et al.* 1998; Chen *et al.* 2008; Mancera *et al.* 2008). The *msh4–R676W* hypomorph was previously identified in the SK1 strain background (Nishant *et al.* 2010) (Figure S1). The SK1 Msh4 protein sequence is different from S288c at one amino acid and from YJM789 at two amino acid positions. Similarly, the SK1 Msh5 protein

Table 1 Spore viability and recombination parameters of the S288c/YJM789 hybrid bearing SK1 *MSH4*/5 or *msh4* mutant alleles

Genotype	*N*	S.V%	Tetrads sequenced	Avg. CO counts ±SD (median)	Avg. NCO counts ±SD (median)
S288c × YJM789	180	84	20	94.4 ± 14.6 (95)	56.8 ± 22.6 (55)
S288c × YJM789 with SK1 *MSH4/MSH5*	209	84	4	85.7 ± 8.5 (83.5)	55.5 ± 6.9 (50)
S288c × YJM789 with SK1 *msh4–R676W/MSH5*	239	76	38	64.2 ± 12.1 (62)	55.2 ± 13.4 (51.5)
S288c × YJM789 *msh4Δ*	100	41	18	49.5 ± 16.7 (47)	69.7 ± 27 (56)

CO, crossover; NCO, noncrossover; *N*, number of tetrads analyzed; SD, standard deviation.

sequence shows polymorphisms relative to S288c at four amino acid and YJM789 at 17 amino acid positions. To avoid a possible incompatibility between Msh4 and Msh5 due to these polymorphisms, we analyzed the *msh4–R676W* hypomorphic mutation in an SK1 context in the S288c/YJM789 hybrid. We introduced the SK1 allele of *MSH5* in the S288c strain-bearing deletion of *msh4Δ*. SK1 *MSH4* and *msh4–R676W* alleles were introduced into the YJM789 strain with *msh5Δ* mutation. The SK1 *MSH4/5* and *msh4–R676W* alleles were analyzed as heterozygotes over their respective null mutations in the S288c/YJM789 hybrid (Figure S2). The S288c/YJM789 hybrid with SK1 *MSH4/5* genes showed high spore viability similar to the wild-type cross (84%) (Table 1). The *msh4–R676W* hypomorph also showed high spore viability of 76% compared to a *msh4Δ* mutant, which has 41% viability in the S288c/YJM789 hybrid (Table 1). To generate high-resolution genome-wide recombination maps in *msh4* mutants and controls, high-coverage whole-genome sequence data were obtained from a total of 80 of the four viable spore tetrads (Table 1 and Table S2). We selected four viable spore tetrads to analyze how variation in crossover frequencies can be tolerated without affecting chromosome segregation. These include 38 tetrads in the *msh4–R676W* hypomorph and 18 tetrads in *msh4Δ*. Among the controls we sequenced 20 tetrads in the S288c/YJM789 hybrid and four tetrads in the S288c/YJM789 hybrid with SK1 *MSH4/5* genes. The sequence data are available from the National Centre for Biotechnology Information Sequence Read Archive under accession no. SRP041856. A total of 58,655 markers were genotyped across the mutant and control strains with a median intermarker interval size of 72 bp (Figure S3). Plots showing segregation information of SNPs in all 80 tetrads sequenced are in File S1. We observed on average 94.4 crossovers in the S288c × YJM789 wild-type strain and 56.8 noncrossovers (Table 1). These values are statistically similar to the crossover (90.4, *t*-test, $P = 0.27$) and noncrossover counts (46.0, *t*-test, $P = 0.05$) observed in the Mancera *et al.* (2008) study. As discussed previously, these numbers do not account for noncrossovers that occur between two consecutive SNP markers or noncrossovers that had restoration repair in the wild-type and *msh4* mutants (Mancera *et al.* 2008). The S288c × YJM789 hybrid with SK1 *MSH4/5* genes had on average 85.7 crossovers and 55.5 noncrossovers (Table 1), which is not significantly different from wild type (*t*-test, $P = 0.22$ for crossovers and $P = 0.88$ for noncrossovers). These results suggest SK1 *MSH4/5* genes are functional in the S288c/YJM789 hybrid with a minor reduction in crossover frequency that does not affect spore viability. The minor reduction in crossover frequency may be because of replacement of the S288c and YJM789 *MSH4/5* alleles with the SK1 *MSH4/5* alleles. Crossover and noncrossover counts for each of the 80 tetrads are shown in Table S3.

The msh4–R676W hypomorph shows a genome-wide decrease in crossing over with high spore viability

We analyzed crossover and noncrossover events in the *msh4–R676W* hypomorph. The average number of crossovers was reduced to 64.2 / meiosis while the noncrossovers were 55.2 / meiosis (Table 1 and Figure 1). The reduction in crossovers compared to wild type is statistically significant for the *msh4–R676W* hypomorph (*t*-test, $P = 4.18 \times 10^{-9}$). Noncrossovers were not statistically different from wild type (*t*-test, $P = 0.77$). These results suggest there is a genome-wide reduction in crossing over in the *msh4–R676W* hypomorph while noncrossovers are similar to wild type. Representative crossover and noncrossover distributions along chromosome IV for wild type and *msh4–R676W* hypomorph are shown in Figure 2, A and B. For the *msh4Δ* mutant, average crossovers were reduced to 49.5 / meiosis (*t*-test, $P = 2.93 \times 10^{-10}$), while noncrossovers (69.7 / meiosis, 56 median) were similar to wild type (*t*-test, $P = 0.12$). The data for *msh4Δ* are consistent with previous analysis of *msh4Δ* tetrads in the S288c x YJM789 hybrid where crossovers showed a twofold reduction while noncrossovers were unchanged (Chen *et al.* 2008; Mancera *et al.* 2008; Oke *et al.* 2014). Collectively these results suggest that in the *msh4–R676W* hypomorph and *msh4Δ* mutant, crossovers are reduced on a genome-wide scale while noncrossovers are maintained (Figure 1). These results suggest that most of the DSBs that cannot be repaired as crossovers in *msh4* mutants are repaired using inter-sister recombination. It is also possible that the restoration/conversion ratio is perturbed in the *msh4* mutants in favor of restoration of the SNP markers so that more noncrossovers are not detected.

To study the effects of chromosome size on crossover distribution, average crossover counts per chromosome were plotted as a function of chromosome size for the wild type, *msh4–R676W* and the *msh4Δ* mutants (Table S4 and Figure 3A). Crossover counts were directly proportional to the chromosome size for wild type with an intercept of 0.98 (95% confidence interval: 0.44, 1.5). For the *msh4–R676W* and *msh4Δ* mutants crossover counts correlated with chromosome

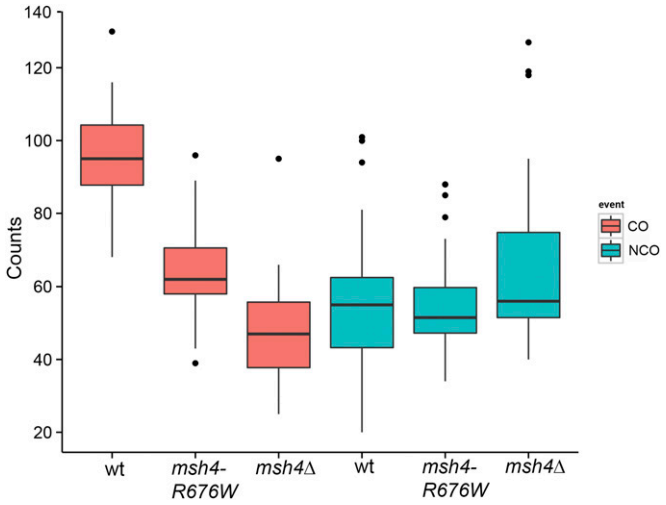

Figure 1 Frequencies of crossovers and noncrossovers per meiosis for wild type, *msh4–R676W*, and *msh4Δ*. Box plots show minimum, first quantile, median, third quantile, and maximum count.

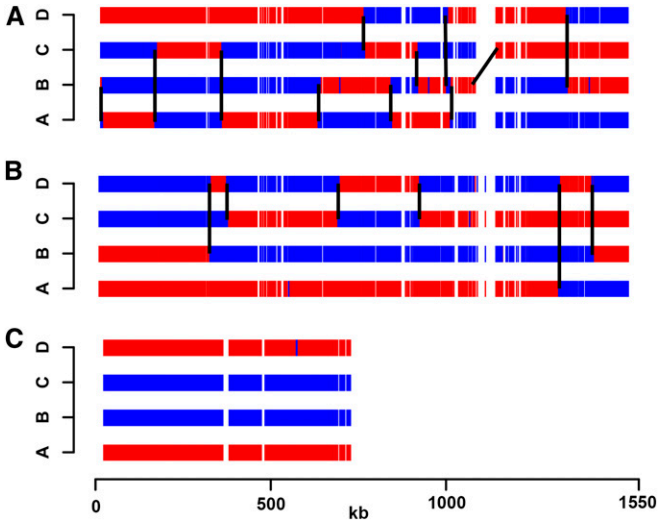

Figure 2 Representative meiotic crossover map for wild-type and *msh4–R676W* mutant. A tetrad showing 11 crossovers on chromosome IV in the wild-type (A) compared to 6 in the *msh4–R676W* mutant (B). (C) *msh4–R676W* tetrad with nonexchange chromosome X. S288c and YJM789 SNPs are shown in blue and red, respectively.

size but with lower intercepts of 0.64 (95% confidence interval: 0.20, 1.1) and 0.59 (95% confidence interval: 0.09, 1.1). Both the *msh4–R676W* and *msh4Δ* mutant showed a proportional loss of crossovers from small and large chromosomes (Figure 3B). These results suggest *msh4* mutations result in similar crossover defects on small and large chromosomes, which could increase the probability of nonexchange events for small chromosomes as discussed later. Noncrossover counts for the wild type, *msh4–R676W* and the *msh4Δ* mutants are also proportional to chromosome size (Table S4 and Figure 3C). While overall noncrossover levels were the same, the *msh4Δ* mutant had statistically significant increase in noncrossover levels on some of the chromosomes (Figure 3D). The noncrossover intercepts for wild type (0.67), *msh4–R676W* (0.94) and *msh4Δ* (1.3) were greater for *msh4* mutants compared to wild type (Figure 3C). The greater noncrossover intercepts in *msh4* mutants compared to wild type maybe due to the increase in noncrossovers on some of the chromosomes in the *msh4* mutants (Figure 3D). Comparison of crossover distribution along the chromosomes showed similar patterns in wild type, *msh4–R676W* and *msh4Δ* mutants (File S2 and Figure S4). Gene conversion information for wild type and *msh4* mutants is shown in File S3.

Crossover reduction is associated with reduced crossover interference in the msh4–R676W hypomorph

Interference limits crossover number and ensures that crossover events are widely spaced along the chromosome (Muller 1916; Hillers 2004; Kleckner *et al.* 2004; Stahl *et al.* 2004). Crossover interference was calculated by modeling the interchromosome distances as a gamma distribution. The gamma distribution is characterized by the shape parameter (γ) and the scale parameter (β). $\gamma = 1$ corresponds to no interference, while $\gamma > 1$ indicates positive interference (Anderson *et al.* 2011). Larger values of γ suggest stronger interference making the method suitable for quantitative analysis of interference instead of just indicating presence or loss of interference. To compare interference between wild type and *msh4* mutants that make fewer crossovers, inter-crossover distances in physical units were converted into genetic distances (cM) to account for differences in crossover numbers (Materials and Methods). For the wild-type strain the γ value was 1.77 which suggests presence of interference. This value is also comparable to the γ value of 1.96 obtained from analysis of inter-crossover distances for 46 wild-type tetrads (Mancera *et al.* 2008; Anderson *et al.* 2011). $\gamma = 0.95$ for *msh4Δ* suggests loss of genetic interference consistent with previous analysis of crossover data at specific loci and genome-wide (Novak *et al.* 2001; Argueso *et al.* 2004; Chen *et al.* 2008; Mancera *et al.* 2008). For *msh4–R676W*, $\gamma = 1.23$ that suggests a moderate loss of interference. The median inter-crossover distances in wild type, *msh4–R676W* and *msh4Δ* were 37.6 cM, 30.3 cM and 20 cM respectively consistent with reduction in inter-crossover distances caused by loss of interference (Figure 4). These differences in inter-crossover distances between *msh4–R676W vs.* wild type ($P = 3.33 \times 10^{-11}$); *msh4–R676W vs. msh4Δ* ($P = 7.18 \times 10^{-10}$) and wild type *vs. msh4Δ* ($P = 2.2 \times 10^{-16}$) are statistically significant using the Wilcoxon rank-sum test. The reduction in interference with reduced crossovers in the *msh4–R676W* hypomorph is consistent with the two pathway model for crossover formation (Stahl *et al.* 2004; Getz *et al.* 2008). The simultaneous loss of crossovers and interference has mechanistic consequences for the maintenance of crossover assurance in the *msh4–R676W* hypomorph (see next section).

Chromatid interference was measured as the ratio of observed and expected two, three and four strand double crossovers events between two adjacent intervals. Chi-square tests show no chromatid interference ($P > 0.05$ for

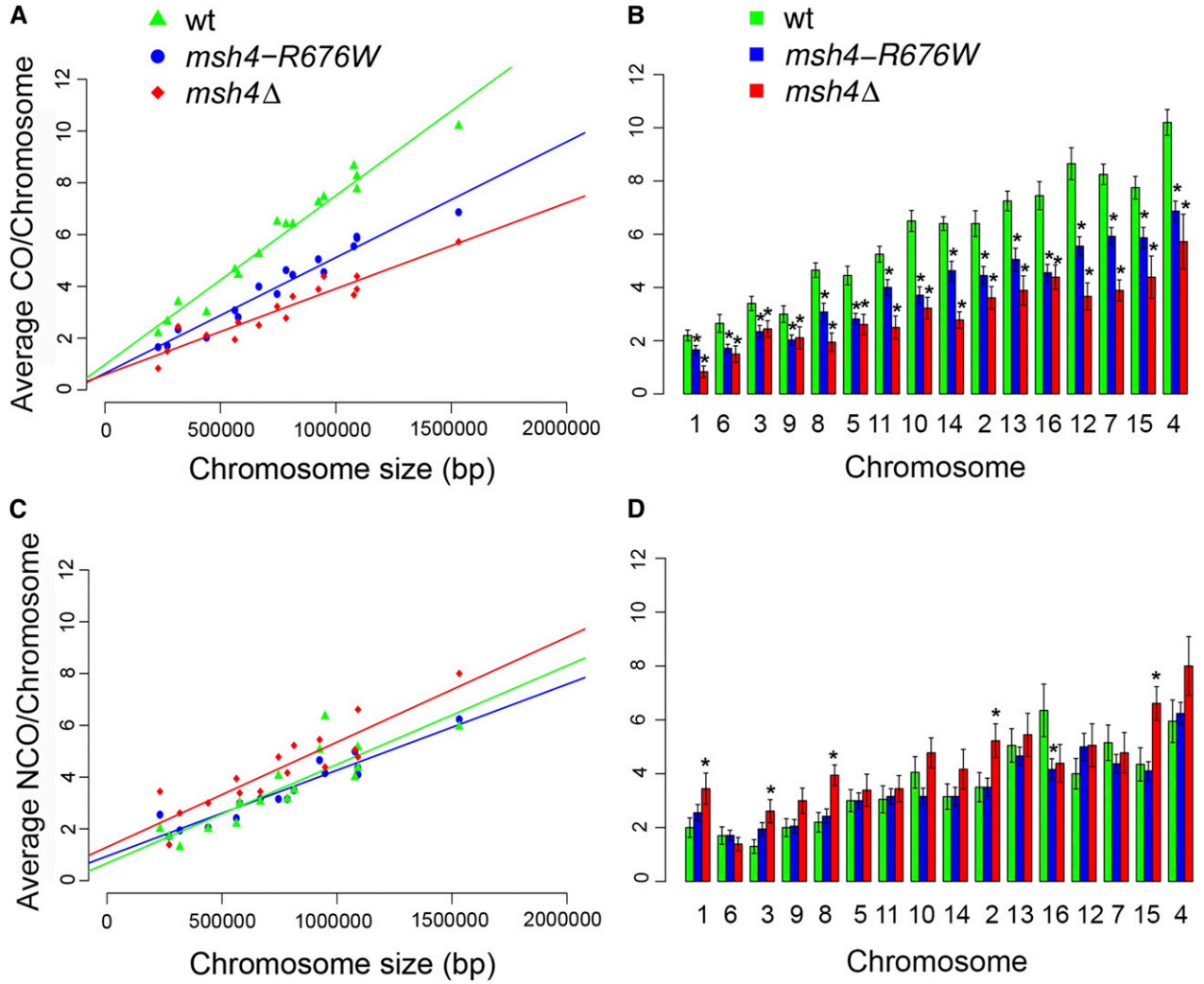

Figure 3 Average crossover and noncrossover counts per chromosome for wild type, *msh4–R676W*, and *msh4Δ*. (A and C) Scatter plot of average crossover and noncrossover counts per chromosome against chromosome size for wild type, *msh4–R676W*, and *msh4Δ*. Best fit line is obtained through linear regression analysis. The equations for the best fit lines are: wild type (CO = 0.0000065 × chr. size + 0.98; NCO = 0.0000034 × chr. size + 0.67), *msh4–R676W* (CO = 0.0000045 × chr. size + 0.64; NCO = 0.0000033 × chr. size + 0.94), *msh4Δ* (CO = 0.0000033 × chr. size + 0.59, NCO = 0.0000041 × chr. size + 1.29). (B and D) Bar plot of average crossover and noncrossover counts per chromosome for wild type, *msh4–R676W*, and *msh4Δ*. Chromosomes (*msh4–R676W* and *msh4Δ*) with significant difference (two-tailed *t*-test for difference in mean; $P < 0.05$) in crossover/noncrossover counts compared to wild type are shown with an asterisk symbol (*). Chromosomes are ordered according to size from left to right. Error bars are mean ±SE.

wild type, *msh4–R676W* and *msh4Δ* mutants suggesting no difference between observed and expected counts) (Table S5). Absence of chromatid interference is also observed for other *zmm* mutants (*zip1Δ*, *zip2Δ*, *zip3Δ*, *zip4Δ*, *spo16Δ*) (Chen *et al.* 2008).

Nonexchange chromosomes are frequent in the msh4–R676W hypomorph

The *msh4–R676W* hypomorph shows genome-wide reduction in crossover number compared to wild type (Figure 1, Table 1, and Table S4). However, this mutant has high spore viability compared to *msh4Δ* (Nishant *et al.* 2010) (Table 1). One mechanism by which the *msh4–R676W* hypomorph can maintain such high spore viability is by distributing the remaining crossovers among all 16 chromosomes to ensure one crossover per homolog pair. The presence of an obligatory crossover on every homolog will be sufficient to ensure high spore viability. When we examined the distribution of crossovers on all chromosomes in the *msh4–R676W* hypomorph, 42% of the tetrads had at least one (39%) or more (3%) nonexchange chromosomes (Table S3). An example of an *msh4–R676W* tetrad with a single nonexchange chromosome is shown in Figure 2C. In the wild-type strain only two of the 20 tetrads sequenced (10%) had a single nonexchange event consistent with the low number of tetrads with nonexchange chromosomes reported previously for wild-type cells (Chen *et al.* 2008; Mancera *et al.* 2008). In the *msh4Δ* mutant 72% of the four viable spore tetrads

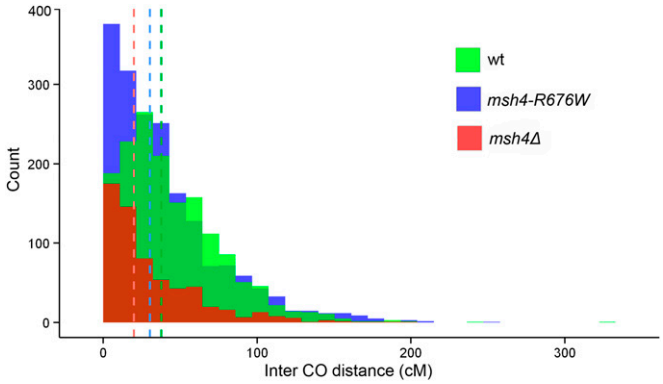

Figure 4 Histogram of intercrossover distances in centimorgans for wild type, *msh4–R676W*, and *msh4Δ*. The vertical lines indicate the median intercrossover distance for wild type, *msh4–R676W*, and *msh4Δ*.

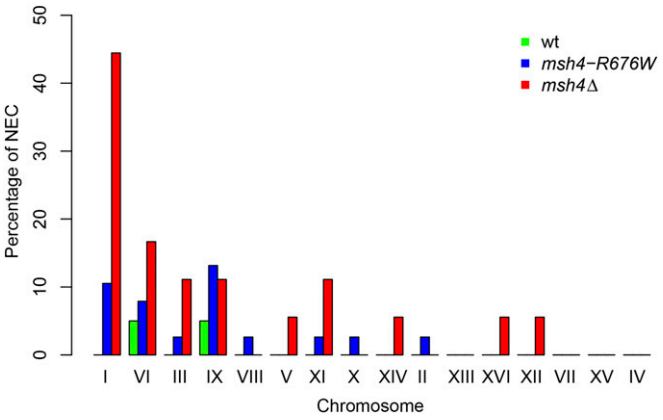

Figure 5 Bar plot showing the percentage of nonexchange chromosomes separately for each chromosome. The data are generated from the analysis of 20 wild-type, 38 *msh4–R676W*, and 18 *msh4Δ* tetrads in the S288c/YJM789 hybrid background. Chromosomes are arranged in increasing order of size.

examined had one (39%) or more than one (33%) nonexchange event. Nonexchange chromosomes have been previously observed among the four viable spore tetrads of other *zmm* mutants including the *msh4Δ* mutant (Chen *et al.* 2008). The percentage of tetrads with more than one nonexchange event (33%) was significantly higher ($P = 0.003$, Fisher's exact test) in *msh4Δ* mutants compared to the *msh4–R676W* hypomorph (3%). Sometimes adjacent crossovers that are closely spaced may be annotated as double noncrossovers inflating the number of nonexchange chromosomes. This problem is more likely to occur in meiotic mutants with reduced or no interference. We inspected each nonexchange chromosome in the wild-type and the *msh4* mutants for ambiguity in the annotation for double crossovers and double noncrossovers and did not find any significant difference in our estimate of nonexchange chromosomes (Table S6). The nucleotide divergence between the S288c and YJM789 strains might also contribute to a small degree of loss of crossover assurance in the S288c/YJM789 hybrid as fewer E0s are observed in other *S. cerevisiae* strains (Kaback *et al.* 1989; Lao *et al.* 2013).

To analyze the influence of chromosome size on occurrence of nonexchange chromosomes in the wild-type, *msh4–R676W*, and *msh4Δ* mutant, we determined the percentage of nonexchange events for each chromosome (Figure 5 and Table S7). Small chromosomes I, III, VI, and IX were observed to have nonexchange events in all three genotypes (wild type, *msh4–R676W*, and *msh4Δ*). Nonexchange events were observed on medium chromosomes II, V, VIII, X, XI, and XIV only in *msh4–R676W* and *msh4Δ*. For large chromosomes IV, VII, XII, XIII, XV, and XVI, nonexchange events occurred only in *msh4Δ*. These observations suggest that minor variations in crossover frequencies are sufficient to produce nonexchange events on small chromosomes. But for medium and large chromosomes, stronger reductions in crossover frequency as observed with the *msh4–R676W* and *msh4Δ* genotypes are required. If all chromosomes are equally likely to receive no crossovers, then a quarter of the E0's are expected to be small chromosomes. We observed 30 of the 40 E0's to be small chromosomes and this indicates an overrepresentation of small chromosomes among E0's ($P = 4.6 \times 10^{-11}$, Binomial test). These results suggest that nonexchange chromosome formation is influenced by chromosome size and small chromosomes are at the greatest risk for loss of crossover assurance when crossover frequencies decrease. Higher frequency of nonexchange events on smaller chromosomes compared to large chromosomes has been observed in other crossover defective mutants and also in human meiosis (Chen *et al.* 2008; Fledel-Alon *et al.* 2009). It is also observed that chromosome I shows a disproportionately high percentage of E0's and the strongest crossover defects in the *msh4Δ* mutant (Figure 3B, Figure 5, and Table S4). The chromosome I-specific defects observed in *msh4Δ* may be because it is the smallest chromosome and therefore sensitive to loss of crossovers. Chromosome I was also observed to have the highest number of nonexchange events in *zmm* mutants in an earlier study by Chen *et al.* (2008). Analysis of copy-number variation using read-depth information did not detect aneuploidy in any of the 80 sequenced tetrads (*Materials and Methods*, data not shown).

To test if the observed number and pattern of nonexchange chromosomes can be predicted from the average crossover counts per chromosome, we modeled the crossover distribution for wild-type and *msh4* mutants using a Poisson distribution (Table 2). The expected number of E0's (fraction of chromosomes with zero crossover) per tetrad were 0.3, 0.8, and 1.4 for wild type, *msh4–R676W*, and *msh4*Δ, respectively (Table 2). Nonexchange chromosomes are therefore expected in *msh4–R676W* if the reduction in crossovers is associated with loss of interference (the Poisson distribution assumes that the crossover events are independent). We compared the expected and observed E0 counts for wild type, *msh4–R676W*, and *msh4Δ*. The observed E0 count per cell in wild type (0.1) is three times lower due to the presence of interference. The observed E0

count per cell in *msh4–R676W* (0.45) is two times lower due to partial loss of interference. For *msh4Δ* there is close concordance between the observed E0 per cell (1.2) and the expected E0 (1.4) as crossover distribution is random. These observations suggest convergence between the expected and observed E0s with diminishing interference (File S4). The presence of interference decreases the proportion of E0's for the same number of crossovers suggesting a mechanistic role for interference in crossover assurance (File S4). Our calculations suggest that in the complete absence of interference, *S. cerevisiae* will require a random distribution of up to 200 crossovers to achieve a 0.98 probability of observing no nonexchange chromosomes (File S4). The Poisson model also suggests that the probability of occurrence of nonexchange events in wild type, *msh4–R676W*, and *msh4Δ* is influenced by chromosome size (Table 2) supporting the experimental observations (Figure 5). Further, the presence of the obligate crossover will also cause the observed E0 frequency to be less than the E0 frequency expected from a random Poisson distribution. We see this trend for the wild type (Table 2). But for the *msh4* mutants the observed E0 frequencies are closer to the expected E0 frequency suggesting loss of the obligate crossover. We did a similar analysis by modeling the noncrossover distribution for wild-type and *msh4* mutants using a Poisson distribution (Table S8). Since noncrossovers do not show interference (Mancera *et al.* 2008), we expect that the observed number of chromosomes without a noncrossover should be close to that predicted from a Poisson distribution. The observed frequency of chromosomes with zero noncrossovers per cell for wild type (1.2), *msh4–R676W* (1.1), and *msh4Δ* (0.77) was greater than the expected frequency (1.07, 0.89, and 0.55 for wild type, *msh4–R676W*, and *msh4Δ,* respectively) (Table S8). These results suggest that there is no obligate noncrossover in the wild type or *msh4* mutants. We looked at the distribution of all gene conversion events not associated with crossovers for the exchange and nonexchange chromosomes in wild type, *msh4–R676W*, and *msh4Δ* (Table S9). The nonexchange chromosomes received 75% of the gene conversions compared to chromosomes with a crossover (P = 0.02). This observation suggests that crossover-independent recombination interactions are less favored for nonexchange chromosomes. Reduced gene conversion events have been observed previously on nonexchange chromosome III in the *dmc1 hed1* mutant by Lao *et al.* (2013).

Nonexchange chromosomes are efficiently segregated in the msh4–R676W hypomorph

Given the large number of E0 chromosomes in the *msh4–R676W* hypomorph we examined how the high spore viability is maintained. We tested the role of specific crossover-independent mechanisms for nonexchange chromosome segregation such as the spindle checkpoint and the contribution of random segregation. Spindle checkpoint proteins Mad2 and Mad3 are known to be involved in nonexchange chromosome segregation (Shonn *et al.* 2000; Cheslock *et al.* 2005; Lacefield and Murray 2007). Mad2 causes a metaphase delay in response to inappropriate microtubule attachment. Mad3 causes a prophase delay in every meiosis to properly align any nonexchange chromosomes to the bipolar spindle (Cheslock *et al.* 2005). We deleted *MAD2* and *MAD3* genes in the *msh4* mutant background in the S288c/YJM789 hybrid to check whether these proteins contribute to the high spore viability observed in the *msh4–R676W* hypomorph. *mad2Δ* and *mad3Δ* single mutants have viability of 39 and 83%, respectively (Table 3 and Figure S5). Double mutants *mad3*Δ *msh4–R676W* and *mad3*Δ *msh4*Δ showed viability of 69 and 38%. When *mad2Δ* mutant was analyzed with *msh4* mutants, the double mutants *mad2*Δ *msh4–R676W* and *mad2Δ msh4Δ* showed viability of 27 and 10%, respectively. The observed double mutant viability of the *msh4* mutants with *mad2Δ* or *mad3Δ* was not significantly different from the expected viability of the double mutants assuming a multiplicative model for the genetic interaction (Table 3; Dixon *et al.* 2009). These results suggest absence of significant negative genetic interaction between the *msh4* mutants and *mad2Δ*, *mad3Δ* mutants. Therefore the spindle checkpoint has only a minor role in the high spore viability of the *msh4–R676W* hypomorph, but other crossover-independent mechanisms might still contribute (see *Discussion*).

We tested whether random segregation of the nonexchange chromosomes can explain the spore viability observed in the *msh4–R676W* hypomorph. We calculated the expected four and two spore viability based on E0 numbers for *msh4–R676W* and *msh4Δ* assuming random segregation (Table 4). For *msh4Δ* there is no difference between the expected (24%) and observed four viable spore class (24%). For *msh4–R676W* an 11% increase in the observed four viable spore class (54%) compared to the expected (47%) is seen. The difference between the observed four viable spore frequency and expected frequency from random segregation is statistically significant for *msh4–R676W* (P = 0.018, one-sided binomial test). For the two viable spore class, the difference between expected and observed viability for *msh4Δ* (41 and 20%, respectively) and *msh4–R676W* (30 and 15%, respectively) is twofold, which suggests efficient segregation of the nonexchange chromosomes at MI. It is also possible that the two viable spore class is underpopulated because there are more zero viable spores. Overall these results suggest that crossover-independent mechanisms enhance the fidelity of chromosome segregation in the *msh4* hypomorph, significantly more than random segregation.

Previous estimates of the efficiency of segregation of nonexchange homeologous/nonhomologous or artificial chromosome pairs in *S. cerevisiae* have ranged from 75 to 90% (Dawson *et al.* 1986; Mann and Davis 1986; Guacci and Kaback 1991; Ross *et al.* 1996; Kemp *et al.* 2004; Cheslock *et al.* 2005; Gladstone *et al.* 2009; Newnham *et al.* 2010). These disjunction estimates are significantly more than the disjunction efficiency observed in the *msh4* mutants. The higher disjunction frequency observed for the nonexchange chromosomes in these studies (Dawson *et al.* 1986; Mann

Table 2 Expected poisson probabilities of observing a nonexchange chromosome given the average crossovers per chromosome

Chromosome	Probability of zero crossover in wild type	Probability of zero crossover in *msh4–R676W*	Probability of zero crossover in *msh4Δ*
I	0.11	0.19	0.44
II	0.00	0.01	0.03
III	0.03	0.10	0.09
IV	0.00	0.00	0.00
V	0.01	0.06	0.07
VI	0.07	0.18	0.22
VII	0.00	0.00	0.02
VIII	0.01	0.05	0.14
IX	0.05	0.13	0.12
X	0.00	0.02	0.04
XI	0.01	0.02	0.08
XII	0.00	0.00	0.03
XIII	0.00	0.01	0.02
XIV	0.00	0.01	0.06
XV	0.00	0.00	0.01
XVI	0.00	0.01	0.01
Expected frequency of E0 chromosomes per cell	0.30	0.80	1.39
Observed frequency of E0 chromosomes per cell	0.1	0.45	1.2

The probability of nonexchange events are chromosome size dependent. Small chromosomes show higher probability of nonexchange events in wild type while small and medium chromosomes show higher probability of nonexchange events in *msh4–R676W* and *msh4Δ*. The expected Poisson probability of observing no crossover on a chromosome was calculated using the mean number of crossovers observed for that particular chromosome (λ) from experimental data and the formula: $P(k) = \lambda^k e^{-\lambda}/k!$. For example, since the mean number of crossovers on chromosome III is 3.4, the expected probability of no crossovers ($k = 0$), is $P(k = 0 \mid \text{mean crossover} = 3.4) = e^{-3.4} = 0.03$.

and Davis 1986; Guacci and Kaback 1991; Ross *et al.* 1996; Kemp *et al.* 2004; Cheslock *et al.* 2005; Gladstone *et al.* 2009; Newnham *et al.* 2010) may be because of the use of a single homeologous/nonhomologous/artificial nonexchange chromosome, which is better segregated by crossover-independent pathways compared to the heterogeneous pool of natural nonexchange chromosomes in the *msh4* mutants (Figure 5). It is also important to note that recombination interactions involving gene conversions will be absent from the nonhomologous or artificial chromosomes used to study nonexchange chromosome segregation.

Discussion

Although the *msh4–R676W* hypomorph makes sufficient crossovers (64/meiosis) to ensure the obligate crossover, crossover assurance was disrupted due to decreased crossover interference. Nonexchange chromosomes are observed in 42% of the meiotic events analyzed. These observations support a mechanistic role for interference in the formation of obligatory crossovers. Genome-wide analysis of crossovers in other meiotic mutants where obligate crossovers are assumed from spore viability or localized measures of crossing over may be necessary to verify any aspect of crossover assurance.

Why is crossover assurance perturbed in the msh4–R676W hypomorph?

Wild-type *S. cerevisiae* meiosis is thought to have a mechanism for crossover assurance, which ensures that one crossover per homolog pair will be maintained (Bishop and Zickler 2004; Shinohara *et al.* 2008). The presence of crossover assurance is supported by (a) the low frequency of nonexchange chromosomes in wild-type *S. cerevisiae* meiosis (Kaback *et al.* 1989; Chen *et al.* 2008; Mancera *et al.* 2008; Shinohara *et al.* 2008) and (b) the phenomenon of crossover homeostasis that maintains crossover number when DSB levels are reduced (Martini *et al.* 2006). This study, as well as previous genome-wide crossover mapping studies, suggests that wild-type strains do maintain crossover assurance although nonexchange chromosomes are occasionally seen (Mancera *et al.* 2008). However, in *msh4–R676W*, 42% of the meioses had at least one nonexchange chromosome. Why does crossover assurance not work in the *msh4–R676W* hypomorph with 64 crossovers and only 16 chromosomes? One reason is that *msh4* mutants show significant reduction in crossovers across all chromosomes, making it possible that small chromosomes do not receive an obligate crossover in every meiosis (Figure 3B). Previous analyses of crossing over at specific loci in *msh4/5* hypomorphs as well as *msh4/5Δ* mutants have suggested a chromosome size effect that is different from our results. Crossover defects were observed in these studies to be stronger on the larger chromosomes compared to the small chromosomes (Abdullah *et al.* 2004; Stahl *et al.* 2004; Nishant *et al.* 2010). This may be due to the small number of loci analyzed on a few chromosomes and highlights the need to look at crossover defects globally to discern chromosome-specific patterns.

The other reason that contributes to the loss of crossover assurance in the *msh4–R676W* hypomorph is the partial loss of interference (Figure 4). In other organisms with a lower number of total crossovers, the interference observed is much higher, such as in *Drosophila* ($\gamma = \sim 4$) and mouse ($\gamma = \sim 10$) (Foss and Stahl 1995; Broman *et al.* 2002; de Boer *et al.* 2006), supposedly to ensure the obligate crossover.

Table 3 Analysis of genetic interaction of mutations in spindle checkpoint genes (*mad2Δ*, *mad3Δ*) with *msh4* mutants

Genotype	*N*	Expected viability (%)	Observed viability (%)	*P*-value (χ^2 test)
Wild type	180		84	
mad2Δ	140		39	
msh4Δ	100		41	
msh4–R676W	239		76	
mad2Δ msh4Δ	120	16	10	$P = 0.09$
mad2Δ msh4–R676W	140	30	27	$P = 0.49$
mad3Δ	60		83	
mad3Δ msh4Δ	60	34	38	$P = 0.76$
mad3Δ msh4–R676W	140	63	69	$P = 0.17$

All mutants are analyzed in the S288c/YJM789 background. *N* is the number of tetrads analyzed. *P*-values indicate statistical significance of the difference between expected and observed viability of the double-mutant combinations The expected spore viability for the double mutants is calculated as the product of the spore viabilities of the individual single mutants (Dixon *et al.* 2009).

S. cerevisiae ($\gamma = 1.77$) has reduced interference compared to these organisms and as a consequence the distribution of crossovers in *S. cerevisiae* is closer to that of a Poisson distribution. The reduced interference may explain why up to 90 crossovers are required to ensure an obligate crossover on every homolog pair for a system with only 16 homolog pairs (File S4). The presence of occasional nonexchange chromosomes in wild-type strains (this study, Mancera *et al.* 2008) may also be due to the reduced stringency of crossover distribution mechanisms in *S. cerevisiae* compared to other model systems. Any reduction in crossovers through a mutation/ polymorphism or random fluctuation in crossover numbers coupled with the loss of interference therefore results in increased incidence of nonexchange pairs.

The alternate possibility is that Msh4/5 has a role in crossover assurance that is compromised in the *msh4–R676W* hypomorph. Since the crossover/noncrossover decision is made before the action of ZMM proteins, the proper execution of the crossover decision might require the wild-type activity of the Msh4/5 proteins (Hunter and Kleckner 2001; Bishop and Zickler 2004; Storlazzi *et al.* 2010). So in the *msh4–R676W* hypomorph the crossovers are not made at the designated sites and hence crossover assurance is perturbed.

How efficiently are natural nonexchange chromosomes segregated in S. cerevisiae?

Nonexchange chromosomes may be segregated randomly or through mechanisms such as centromere pairing, the spindle checkpoint, or heterochromatin association that facilitate accurate segregation (Li and Murray 1991; Dernburg *et al.* 1996; Shonn *et al.* 2000; Kemp *et al.* 2004). Crossover-independent meiotic chromosome segregation has been analyzed previously in *S. cerevisiae*, *Schizosaccharomyces pombe*, and *Drosophila* (Sturtevant and Beadle 1936; Carpenter 1973; Dawson *et al.* 1986; Mann and Davis 1986; Davis and Smith 2003). In *S. cerevisiae*, centromere pairing (mediated by Zip1) is thought to decrease rotational freedom of the homologous kinetochores and ensure that they attach to microtubules from opposite poles (Ostergren 1951; Lacefield and Murray 2007; Gladstone *et al.* 2009; Newnham *et al.* 2010; Obeso *et al.* 2013). The spindle checkpoint is activated in response to improper or unattached kinetochores (Li and Murray 1991; Rieder *et al.* 1994; Li and Nicklas 1995). Improper spindle-kinetochore attachments are common in case of nonexchange chromosomes. Spindle checkpoint genes *MAD1*, *MAD2*, *MAD3* have been shown to facilitate segregation of nonexchange pairs in *S. cerevisiae* or chromosome pairs with crossovers placed far from the centromere (Shonn *et al.* 2000; Cheslock *et al.* 2005; Lacefield and Murray 2007). Cell-cycle delays introduced by *MAD1* (metaphase I), *MAD2* (metaphase I), and *MAD3* (prophase I) are thought to provide additional time for chromosome pairs to establish bipolar attachment of spindles to kinetochores (Cheslock *et al.* 2005). These backup pathways can mask defects in crossover assurance. Analysis of genetic interactions between the *msh4–R676W* hypomorph and spindle checkpoint genes *MAD2*, *MAD3* suggest that the spindle checkpoint is not critical for proper segregation of the nonexchange homologous chromosomes in the *msh4–R676W* hypomorphic background, but other mechanisms might still play a role.

For example, the high spore viability of the *msh4–R676W* hypomorph can also be explained by a role for the Msh4/5 proteins in nonexchange chromosome segregation, which is distinct from its pro-crossover role. The predicted early roles of Msh4/5 proteins in homologous pairing supports such a possibility (Storlazzi *et al.* 2010). The *msh4–R676W* hypomorph might be proficient in such chromosome segregation functions but not able to execute crossover formation. A possible role for the Msh4/5 complex in segregation of nonexchange chromosomes can also explain why the *mlh3Δ mms4Δ* double mutant make very few crossovers but has good viability (Argueso *et al.* 2004; Brown *et al.* 2013). These mechanisms need not be mutually exclusive and may all contribute to the efficiency of nonexchange chromosome segregation.

Our study also sheds light on how many nonexchange chromosomes can be efficiently segregated. In the *msh4–R676W* hypomorph, only 3% of the meiosis had more than one nonexchange chromosome compared to 33% in *msh4Δ* mutants. But in none of the cases we found more than three nonexchange chromosomes in a given meiosis (Table S3). These results support the idea that there are limits on how many nonexchange chromosomes can be handled. With four E0's per meiotic cell, the expected four viable spore class from random segregation will be close to 6% (1 of 2^4 tetrads will contain four viable spores), which may not be observable unless large number of tetrads are analyzed. The presence of multiple nonexchange chromosomes may be the reason crossover-independent pathways cannot improve spore viability in *msh4Δ* mutants.

Chromosome size and shape have a role in nonexchange chromosome segregation in *Drosophila* (Grell 1964; Hawley *et al.* 1992). In *S. cerevisiae*, analysis of segregation of nonhomologous natural chromosomes and a centromere plasmid showed absence of shape and size bias (Guacci and Kaback

Table 4 Calculation of estimated four viable and two viable spore tetrads based on E0 counts

	Wild type		*msh4–R676W*		*msh4Δ*	
No. of E0 chromosomes	No. of tetrads	Expected number of nonviable tetrads	No. of tetrads	Expected number of nonviable tetrads	No. of tetrads	Expected number of nonviable tetrads
0	18	0	22	0	5	0
1	2	2	15	15	7	7
2	0	0	1	3	4	12
3	0	0	0	0	2	14
Total	20	2	38	18	18	33
Expected fraction of four viable spore tetrads		0.91		0.68		0.35
Observed fraction of four viable spore tetrads		0.63				
Fraction of four viable spore tetrads expected after correction				0.47		0.24
Observed four viable spore tetrads				54%		24%
Fraction of expected two viable spore tetrads		0.09		0.3		0.41
Observed two viable spore tetrads		10%		15%		20%

We calculated the expected number of four viable spore tetrads based on the proportion of nonviable tetrads that arise due to mis-segregation of chromosomes. Assuming random segregation of nonexchange chromosomes, if we observe one tetrad with one nonexchange chromosome, we expect there is one other nonviable tetrad (*i.e.*, not four viable spore tetrad). Likewise for one tetrad with two nonexchange chromosomes we expect 2^2 - 1 = 3 other nonviable tetrads and for one tetrad with three nonexchange chromosomes, one expects 2^3 - 1 = 7 other non-four viable spore tetrads. We can then estimate the expected number of four viable spore tetrads for each genotype by dividing the observed count of four viable spore tetrads over the total (expected number of nonviable tetrads + observed four viable spore tetrads). After obtaining this expected proportion, we scaled it down by the fraction observed in wild type (0.90 / 0.63) to obtain a corrected estimate. A similar logic is used to calculate the expected number of two viable spore tetrads.

1991). Similar results were observed with the segregation analysis of artificial nonexchange chromosomes that are of comparable or different sizes within a twofold range (Ross *et al.* 1996). These studies may have failed to detect the effect of chromosome size on segregation of natural nonexchange *S. cerevisiae* chromosomes. Our analysis using *msh4* mutants indicates that chromosome size might play some role in nonexchange segregation (Figure 5 and Table 2). In the *msh4–R676W* hypomorph, nonexchange events are mainly restricted to small and medium-sized chromosomes as predicted from the Poisson probabilities of observing a nonexchange chromosome (Table 2). Whereas in *msh4*Δ mutants nonexchange events are found on small, medium, and large chromosomes. We hypothesize that the viability defect found in *msh4*Δ mutants could be due to the presence of nonexchange events on large chromosomes. Crossover-independent mechanisms might be efficient in segregating small and medium-sized nonexchange chromosomes, whereas the process may be less efficient with large chromosomes.

A major challenge in studying achiasmate chromosome segregation mechanisms is that most of the mutants that generate natural nonexchange chromosomes have very poor spore viability. Some exceptions include the *msh4–R676W* hypomoprh (this study) or *mlh3Δ mms4Δ* mutants that show a 6- to 17-fold reduction in crossing over at specific loci (Brown *et al.* 2013). On the other hand, wild-type cells have high frequencies of crossovers that result in very few achiasmate chromosomes (Kaback *et al.* 1992). Cytological approaches that do not require viable spores are one alternative. We suggest that the *msh4–R676W* hypomorph can be used to study the efficiency of crossover-independent segregation mechanisms as it has a large number of meioses with nonexchange chromosomes and still maintains high spore viability.

To conclude, we used the baker's yeast *Saccharomyces cerevisiae* as a model to study whether the obligate crossover is insulated from variation in crossover numbers. An *S. cerevisiae msh4–R676W* hypomorphic allele that has crossover defects but maintains good viability was used to experimentally induce variation in crossover numbers. The *msh4–R676W* hypomorph showed ~30% genome-wide reduction in crossovers and reduced crossover interference. Statistically significant reduction in crossover numbers was observed on all chromosomes in the *msh4* mutants. Crossover assurance was lost in 42% of the meioses in the *msh4–R676W* hypomorph, especially on small and medium-sized chromosomes that were most sensitive to even minor fluctuations in crossover number. Since Msh4/5 is part of the ZMM complex, the loss of assurance in *msh4–R676W* may also be in part due to the direct role of Msh4/5 in crossover assurance. The distribution of nonexchange chromosomes observed in *msh4* mutants was consistent with predictions based on modeling the crossovers as a Poisson distribution and provides a mechanistic link between interference and the obligate crossover. The high spore viability of the *msh4–R676W* hypomorph is maintained by efficient segregation of a limited number of nonexchange chromosomes. Our results suggest that variation in crossover frequencies can disrupt obligate crossover formation without affecting viability. Such nonexchange chromosomes may be more common than previously thought and highlight the need to use genome-wide crossover mapping methods to analyze crossover assurance.

Acknowledgments

We thank Eric Alani, Michael Lichten, and Eugenio Mancera for critical reading of the manuscript and helpful discussions. We also thank Jennifer Fung for suggestions on using the ReCombine suite of programs. This study was technically supported by the European Molecular Biology Laboratory Genomics Core Facility (GeneCore). K.T.N. is supported by a Wellcome Trust-Department of Biotechnology (DBT) India Alliance Intermediate fellowship (IA/I/11/2500268) and Indian Institute of Science Education and Research Thiruvananthapuram (IISER-TVM) intramural funds. The research leading to these results has received funding from the National Institutes of Health and the European Research Council under the European Union's Seventh Framework Programme (FP7/2007-2013)/ ERC Grant agreement no. AdG-294542 to L.M.S. G.N.K. is also supported by a fellowship from the Council for Scientific and Industrial Research, New Delhi. The funders had no role in study design, data collection and interpretation, preparation of the manuscript or decision to publish.

Literature Cited

Abdullah, M. F., E. R. Hoffmann, V. E. Cotton, and R. H. Borts, 2004 A role for the MutL homologue *MLH2* in controlling heteroduplex formation and in regulating between two different crossover pathways in budding yeast. Cytogenet. Genome Res. 107: 180–190.

Agarwal, S., and G. S. Roeder, 2000 Zip3 provides a link between recombination enzymes and synaptonemal complex proteins. Cell 102: 245–255.

Allers, T., and M. Lichten, 2001 Differential timing and control of noncrossover and crossover recombination during meiosis. Cell 106: 47–57.

Anderson, C. M., S. Y. Chen, M. T. Dimon, A. Oke, J. L. DeRisi *et al.*, 2011 ReCombine: a suite of programs for detection and analysis of meiotic recombination in whole-genome datasets. PLoS ONE 6: e25509.

Argueso, J. L., A. W. Kijas, S. Sarin, J. Heck, M. Waase *et al.*, 2003 Systematic mutagenesis of the *Saccharomyces cerevisiae MLH1* gene reveals distinct roles for Mlh1p in meiotic crossing over and in vegetative and meiotic mismatch repair. Mol. Cell. Biol. 23: 873–886.

Argueso, J. L., J. Wanat, Z. Gemici, and E. Alani, 2004 Competing crossover pathways act during meiosis in *Saccharomyces cerevisiae*. Genetics 168: 1805–1816.

Baker, S. M., A. W. Plug, T. A. Prolla, C. E. Bronner, A. C. Harris *et al.*, 1996 Involvement of mouse Mlh1 in DNA mismatch repair and meiotic crossing over. Nat. Genet. 13: 336–342.

Barlow, A. L., and M. A. Hulten, 1998 Crossing over analysis at pachytene in man. Eur. J. Hum. Genet. 6: 350–358.

Berchowitz, L. E., and G. P. Copenhaver, 2010 Genetic interference: don't stand so close to me. Curr. Genomics 11: 91–102.

Bishop, D. K., and D. Zickler, 2004 Early decision; meiotic crossover interference prior to stable strand exchange and synapsis. Cell 117: 9–15.

Borner, G. V., N. Kleckner, and N. Hunter, 2004 Crossover/noncrossover differentiation, synaptonemal complex formation, and regulatory surveillance at the leptotene/zygotene transition of meiosis. Cell 117: 29–45.

Broman, K. W., L. B. Rowe, G. A. Churchill, and K. Paigen, 2002 Crossover interference in the mouse. Genetics 160: 1123–1131.

Brown, M. S., E. Lim, C. Chen, K. T. Nishant, and E. Alani, 2013 Genetic analysis of mlh3 mutations reveals interactions between crossover promoting factors during meiosis in baker's yeast. *G3 Genes Genomes Genet.* 3: 9–22.

Carpenter, A. T., 1973 A meiotic mutant defective in distributive disjunction in *Drosophila melanogaster*. Genetics 73: 393–428.

Chen, S. Y., T. Tsubouchi, B. Rockmill, J. S. Sandler, D. R. Richards *et al.*, 2008 Global analysis of the meiotic crossover landscape. Dev. Cell 15: 401–415.

Cheslock, P. S., B. J. Kemp, R. M. Boumil, and D. S. Dawson, 2005 The roles of *MAD1*, *MAD2* and *MAD3* in meiotic progression and the segregation of nonexchange chromosomes. Nat. Genet. 37: 756–760.

Cheung, V. G., J. T. Burdick, D. Hirschmann, and M. Morley, 2007 Polymorphic variation in human meiotic recombination. Am. J. Hum. Genet. 80: 526–530.

Chowdhury, R., P. R. Bois, E. Feingold, S. L. Sherman, and V. G. Cheung, 2009 Genetic analysis of variation in human meiotic recombination. PLoS Genet. 5: e1000648.

Chua, P. R., and G. S. Roeder, 1998 Zip2, a meiosis-specific protein required for the initiation of chromosome synapsis. Cell 93: 349–359.

Cole, F., L. Kauppi, J. Lange, I. Roig, R. Wang *et al.*, 2012 Homeostatic control of recombination is implemented progressively in mouse meiosis. Nat. Cell Biol. 14: 424–430.

Davis, L., and G. R. Smith, 2003 Nonrandom homolog segregation at meiosis I in *Schizosaccharomyces pombe* mutants lacking recombination. Genetics 163: 857–874.

Dawson, D. S., A. W. Murray, and J. W. Szostak, 1986 An alternative pathway for meiotic chromosome segregation in yeast. Science 234: 713–717.

de Boer, E., P. Stam, A. J. Dietrich, A. Pastink, and C. Heyting, 2006 Two levels of interference in mouse meiotic recombination. Proc. Natl. Acad. Sci. USA 103: 9607–9612.

De Muyt, A., L. Jessop, E. Kolar, A. Sourirajan, J. Chen *et al.*, 2012 BLM helicase ortholog Sgs1 is a central regulator of meiotic recombination intermediate metabolism. Mol. Cell 46: 43–53.

de Vries, S. S., E. B. Baart, M. Dekker, A. Siezen, D. G. de Rooij *et al.*, 1999 Mouse MutS-like protein Msh5 is required for proper chromosome synapsis in male and female meiosis. Genes Dev. 13: 523–531.

Dernburg, A. F., J. W. Sedat, and R. S. Hawley, 1996 Direct evidence of a role for heterochromatin in meiotic chromosome segregation. Cell 86: 135–146.

Dixon, S. J., M. Costanzo, A. Baryshnikova, B. Andrews, and C. Boone, 2009 Systematic mapping of genetic interaction networks. Annu. Rev. Genet. 43: 601–625.

Edelmann, W., P. E. Cohen, B. Kneitz, N. Winand, M. Lia *et al.*, 1999 Mammalian MutS homologue 5 is required for chromosome pairing in meiosis. Nat. Genet. 21: 123–127.

Fledel-Alon, A., D. J. Wilson, K. Broman, X. Wen, C. Ober *et al.*, 2009 Broad-scale recombination patterns underlying proper disjunction in humans. PLoS Genet. 5: e1000658.

Foss, E. J., and F. W. Stahl, 1995 A test of a counting model for chiasma interference. Genetics 139: 1201–1209.

Getz, T. J., S. A. Banse, L. S. Young, A. V. Banse, J. Swanson *et al.*, 2008 Reduced mismatch repair of heteroduplexes reveals "non"-interfering crossing over in wild-type *Saccharomyces cerevisiae*. Genetics 178: 1251–1269.

Gietz, R. D., R. H. Schiestl, A. R. Willems, and R. A. Woods, 1995 Studies on the transformation of intact yeast cells by the LiAc/SS-DNA/PEG procedure. Yeast 11: 355–360.

Gladstone, M. N., D. Obeso, H. Chuong, and D. S. Dawson, 2009 The synaptonemal complex protein Zip1 promotes bi-orientation of centromeres at meiosis I. PLoS Genet. 5: e1000771.

Goldstein, A. L., and J. H. McCusker, 1999 Three new dominant drug resistance cassettes for gene disruption in *Saccharomyces cerevisiae*. Yeast 15: 1541–1553.

Grell, R. F., 1964 Distributive pairing: the size-dependent mechanism for regular segregation of the fourth chromosomes in *Drosophila Melanogaster*. Proc. Natl. Acad. Sci. USA 52: 226–232.

Guacci, V., and D. B. Kaback, 1991 Distributive disjunction of authentic chromosomes in *Saccharomyces cerevisiae*. Genetics 127: 475–488.

Guillon, H., F. Baudat, C. Grey, R. M. Liskay, and B. de Massy, 2005 Crossover and noncrossover pathways in mouse meiosis. Mol. Cell 20: 563–573.

Hawley, R. S., H. Irick, A. E. Zitron, D. A. Haddox, A. Lohe *et al.*, 1992 There are two mechanisms of achiasmate segregation in *Drosophila* females, one of which requires heterochromatic homology. Dev. Genet. 13: 440–467.

Hillers, K. J., 2004 Crossover interference. Curr. Biol. 14: R1036–R1037.

Hollingsworth, N. M., L. Ponte, and C. Halsey, 1995 *MSH5*, a novel MutS homolog, facilitates meiotic reciprocal recombination between homologs in *Saccharomyces cerevisiae* but not mismatch repair. Genes Dev. 9: 1728–1739.

Hunter, N., and N. Kleckner, 2001 The single-end invasion: an asymmetric intermediate at the double-strand break to double-holliday junction transition of meiotic recombination. Cell 106: 59–70.

Kaback, D. B., H. Y. Steensma, and P. de Jonge, 1989 Enhanced meiotic recombination on the smallest chromosome of *Saccharomyces cerevisiae*. Proc. Natl. Acad. Sci. USA 86: 3694–3698.

Kaback, D. B., V. Guacci, D. Barber, and J. W. Mahon, 1992 Chromosome size-dependent control of meiotic recombination. Science 256: 228–232.

Karpen, G. H., M. H. Le, and H. Le, 1996 Centric heterochromatin and the efficiency of achiasmate disjunction in *Drosophila* female meiosis. Science 273: 118–122.

Keeney, S., C. N. Giroux, and N. Kleckner, 1997 Meiosis-specific DNA double-strand breaks are catalyzed by Spo11, a member of a widely conserved protein family. Cell 88: 375–384.

Kemp, B., R. M. Boumil, M. N. Stewart, and D. S. Dawson, 2004 A role for centromere pairing in meiotic chromosome segregation. Genes Dev. 18: 1946–1951.

Kijas, A. W., B. Studamire, and E. Alani, 2003 Msh2 separation of function mutations confer defects in the initiation steps of mismatch repair. J. Mol. Biol. 331: 123–138.

Klambauer, G., K. Schwarzbauer, A. Mayr, D. A. Clevert, A. Mitterecker *et al.*, 2012 cn.MOPS: mixture of Poissons for discovering copy number variations in next-generation sequencing data with a low false discovery rate. Nucleic Acids Res. 40: e69.

Kleckner, N., D. Zickler, G. H. Jones, J. Dekker, R. Padmore *et al.*, 2004 A mechanical basis for chromosome function. Proc. Natl. Acad. Sci. USA 101: 12592–12597.

Kneitz, B., P. E. Cohen, E. Avdievich, L. Zhu, M. F. Kane *et al.*, 2000 MutS homolog 4 localization to meiotic chromosomes is required for chromosome pairing during meiosis in male and female mice. Genes Dev. 14: 1085–1097.

Kolas, N. K., A. Svetlanov, M. L. Lenzi, F. P. Macaluso, S. M. Lipkin *et al.*, 2005 Localization of MMR proteins on meiotic chromosomes in mice indicates distinct functions during prophase I. J. Cell Biol. 171: 447–458.

Kong, A., G. Thorleifsson, D. F. Gudbjartsson, G. Masson, A. Sigurdsson *et al.*, 2010 Fine-scale recombination rate differences between sexes, populations and individuals. Nature 467: 1099–1103.

Kong, A., G. Thorleifsson, M. L. Frigge, G. Masson, D. F. Gudbjartsson *et al.*, 2014 Common and low-frequency variants associated with genome-wide recombination rate. Nat. Genet. 46: 11–16.

Lacefield, S., and A. W. Murray, 2007 The spindle checkpoint rescues the meiotic segregation of chromosomes whose crossovers are far from the centromere. Nat. Genet. 39: 1273–1277.

Langmead, B., C. Trapnell, M. Pop, and S. L. Salzberg, 2009 Ultrafast and memory-efficient alignment of short DNA sequences to the human genome. Genome Biol. 10: R25.

Lao, J. P., V. Cloud, C. C. Huang, J. Grubb, D. Thacker *et al.*, 2013 Meiotic crossover control by concerted action of Rad51-Dmc1 in homolog template bias and robust homeostatic regulation. PLoS Genet. 9: e1003978.

Li, R., and A. W. Murray, 1991 Feedback control of mitosis in budding yeast. Cell 66: 519–531.

Li, X., and R. B. Nicklas, 1995 Mitotic forces control a cell-cycle checkpoint. Nature 373: 630–632.

Lipkin, S. M., P. B. Moens, V. Wang, M. Lenzi, D. Shanmugarajah *et al.*, 2002 Meiotic arrest and aneuploidy in MLH3-deficient mice. Nat. Genet. 31: 385–390.

Lu, S., C. Zong, W. Fan, M. Yang, J. Li *et al.*, 2012 Probing meiotic recombination and aneuploidy of single sperm cells by whole-genome sequencing. Science 338: 1627–1630.

Lynn, A., R. Soucek, and G. V. Borner, 2007 ZMM proteins during meiosis: crossover artists at work. Chromosome Res. 15: 591–605.

Mancera, E., R. Bourgon, A. Brozzi, W. Huber, and L. M. Steinmetz, 2008 High-resolution mapping of meiotic crossovers and non-crossovers in yeast. Nature 454: 479–485.

Mann, C., and R. W. Davis, 1986 Meiotic disjunction of circular minichromosomes in yeast does not require DNA homology. Proc. Natl. Acad. Sci. USA 83: 6017–6019.

Martini, E., R. L. Diaz, N. Hunter, and S. Keeney, 2006 Crossover homeostasis in yeast meiosis. Cell 126: 285–295.

Martini, E., V. Borde, M. Legendre, S. Audic, B. Regnault *et al.*, 2011 Genome-wide analysis of heteroduplex DNA in mismatch repair-deficient yeast cells reveals novel properties of meiotic recombination pathways. PLoS Genet. 7: e1002305.

McCusker, J. H., K. V. Clemons, D. A. Stevens, and R. W. Davis, 1994 Genetic characterization of pathogenic *Saccharomyces cerevisiae* isolates. Genetics 136: 1261–1269.

Mortimer, R. K., and J. R. Johnston, 1986 Genealogy of principal strains of the yeast genetic stock center. Genetics 113: 35–43.

Muller, H. J., 1916 The mechanism of crossing over. Am. Nat. 50: 284–305.

Newnham, L., P. Jordan, B. Rockmill, G. S. Roeder, and E. Hoffmann, 2010 The synaptonemal complex protein, Zip1, promotes the segregation of nonexchange chromosomes at meiosis I. Proc. Natl. Acad. Sci. USA 107: 781–785.

Nishant, K.T., A.J. Plys, and E. Alani, 2008 A mutation in the putative MLH3 endonuclease domain confers a defect in both mismatch repair and meiosis in *Saccharomyces cerevisiae*. Genetics 179: 747–755.

Nishant, K. T., C. Chen, M. Shinohara, A. Shinohara, and E. Alani, 2010 Genetic analysis of baker's yeast Msh4–Msh5 reveals a threshold crossover level for meiotic viability. PLoS Genet. 6: e1001083.

Novak, J. E., P. B. Ross-Macdonald, and G. S. Roeder, 2001 The budding yeast Msh4 protein functions in chromosome synapsis and the regulation of crossover distribution. Genetics 158: 1013–1025.

Obeso, D., R. J. Pezza, and D. Dawson, 2013 Couples, pairs, and clusters: mechanisms and implications of centromere associations in meiosis. Chromosoma 123: 43–55.

Oke, A., C. M. Anderson, P. Yam, and J. C. Fung, 2014 Controlling meiotic recombination repair-specifying the roles of ZMMs, Sgs1 and Mus81/Mms4 in crossover formation. PLoS Genet. 10: e1004690.

Olshen, A. B., E. S. Venkatraman, R. Lucito, and M. Wigler, 2004 Circular binary segmentation for the analysis of array-based DNA copy number data. Biostatistics 5: 557–572.

Ostergren, G., 1951 The mechanism of co-orientation in bivalents and multivalents. Hereditas 37: 156.

Patel, R. K., and M. Jain, 2012 NGS QC Toolkit: a toolkit for quality control of next generation sequencing data. PLoS ONE 7: e30619.

Petronczki, M., M. F. Siomos, and K. Nasmyth, 2003 Un ménage à quatre: the molecular biology of chromosome segregation in meiosis. Cell 112: 423–440.

Qi, J., A. J. Wijeratne, L. P. Tomsho, Y. Hu, S. C. Schuster *et al.*, 2009 Characterization of meiotic crossovers and gene conversion by whole-genome sequencing in *Saccharomyces cerevisiae*. BMC Genomics 10: 475.

Rakshambikai, R., N. Srinivasan, and K. T. Nishant, 2013 Structural insights into *Saccharomyces cerevisiae* Msh4–Msh5 complex function using homology modeling. PLoS ONE 8: e78753.

Rieder, C. L., A. Schultz, R. Cole, and G. Sluder, 1994 Anaphase onset in vertebrate somatic cells is controlled by a checkpoint that monitors sister kinetochore attachment to the spindle. J. Cell Biol. 127: 1301–1310.

Roeder, G. S., 1997 Meiotic chromosomes: it takes two to tango. Genes Dev. 11: 2600–2621.

Rose, M. D., F. Winston, and P. Hieter, 1990 *Methods in yeast genetics*. Cold Spring Harbor Laboratory Press, Cold Spring Harbor, NY.

Ross, L. O., S. Rankin, M. F. Shuster, and D. S. Dawson, 1996 Effects of homology, size and exchange of the meiotic segregation of model chromosomes in *Saccharomyces cerevisiae*. Genetics 142: 79–89.

Ross-Macdonald, P., and G. S. Roeder, 1994 Mutation of a meiosis-specific MutS homolog decreases crossing over but not mismatch correction. Cell 79: 1069–1080.

Rosu, S., D. E. Libuda, and A. M. Villeneuve, 2011 Robust crossover assurance and regulated interhomolog access maintain meiotic crossover number. Science 334: 1286–1289.

Santucci-Darmanin, S., S. Neyton, F. Lespinasse, A. Saunieres, P. Gaudray *et al.*, 2002 The DNA mismatch-repair MLH3 protein interacts with MSH4 in meiotic cells, supporting a role for this MutL homolog in mammalian meiotic recombination. Hum. Mol. Genet. 11: 1697–1706.

Shinohara, M., S. D. Oh, N. Hunter, and A. Shinohara, 2008 Crossover assurance and crossover interference are distinctly regulated by the ZMM proteins during yeast meiosis. Nat. Genet. 40: 299–309.

Shonn, M. A., R. McCarroll, and A. W. Murray, 2000 Requirement of the spindle checkpoint for proper chromosome segregation in budding yeast meiosis. Science 289: 300–303.

Snowden, T., S. Acharya, C. Butz, M. Berardini, and R. Fishel, 2004 hMSH4-hMSH5 recognizes Holliday Junctions and forms a meiosis-specific sliding clamp that embraces homologous chromosomes. Mol. Cell 15: 437–451.

Snowden, T., K. S. Shim, C. Schmutte, S. Acharya, and R. Fishel, 2008 hMSH4–hMSH5 adenosine nucleotide processing and interactions with homologous recombination machinery. J. Biol. Chem. 283: 145–154.

Stahl, F. W., H. M. Foss, L. S. Young, R. H. Borts, M. F. Abdullah *et al.*, 2004 Does crossover interference count in *Saccharomyces cerevisiae?* Genetics 168: 35–48.

Storlazzi, A., S. Gargano, G. Ruprich-Robert, M. Falque, M. David *et al.*, 2010 Recombination proteins mediate meiotic spatial chromosome organization and pairing. Cell 141: 94–106.

Sturtevant, A. H., and G. W. Beadle, 1936 The relations of inversions in the X chromosome of *Drosophila Melanogaster* to crossing over and disjunction. Genetics 21: 554–604.

Tsubouchi, T., H. Zhao, and G. S. Roeder, 2006 The meiosis-specific zip4 protein regulates crossover distribution by promoting synaptonemal complex formation together with zip2. Dev. Cell 10: 809–819.

Wilkening, S., M. M. Tekkedil, G. Lin, E. S. Fritsch, W. Wei *et al.*, 2013 Genotyping 1000 yeast strains by next-generation sequencing. BMC Genomics 14: 90.

Winzeler, E. A., D. R. Richards, A. R. Conway, A. L. Goldstein, S. Kalman *et al.*, 1998 Direct allelic variation scanning of the yeast genome. Science 281: 1194–1197.

Woods, L. M., C. A. Hodges, E. Baart, S. M. Baker, M. Liskay *et al.*, 1999 Chromosomal influence on meiotic spindle assembly: abnormal meiosis I in female Mlh1 mutant mice. J. Cell Biol. 145: 1395–1406.

Zakharyevich, K., Y. Ma, S. Tang, P. Y. Hwang, S. Boiteux *et al.*, 2010 Temporally and biochemically distinct activities of Exo1 during meiosis: double-strand break resection and resolution of double Holliday junctions. Mol. Cell 40: 1001–1015.

Zakharyevich, K., S. Tang, Y. Ma, and N. Hunter, 2012 Delineation of joint molecule resolution pathways in meiosis identifies a crossover-specific resolvase. Cell 149: 334–347.

Zickler, D., and N. Kleckner, 1999 Meiotic chromosomes: integrating structure and function. Annu. Rev. Genet. 33: 603–754.

Communicating editor: N. M. Hollingsworth

GENETICS

Supporting Information
http://www.genetics.org/lookup/suppl/doi:10.1534/genetics.114.172320/-/DC1

Variation in Crossover Frequencies Perturb Crossover Assurance Without Affecting Meiotic Chromosome Segregation in *Saccharomyces cerevisiae*

Gurukripa N. Krishnaprasad, Mayakonda T. Anand, Gen Lin, Manu M. Tekkedil, Lars M. Steinmetz, and Koodali T. Nishant

DOI: 10.1534/genetics.114.172320

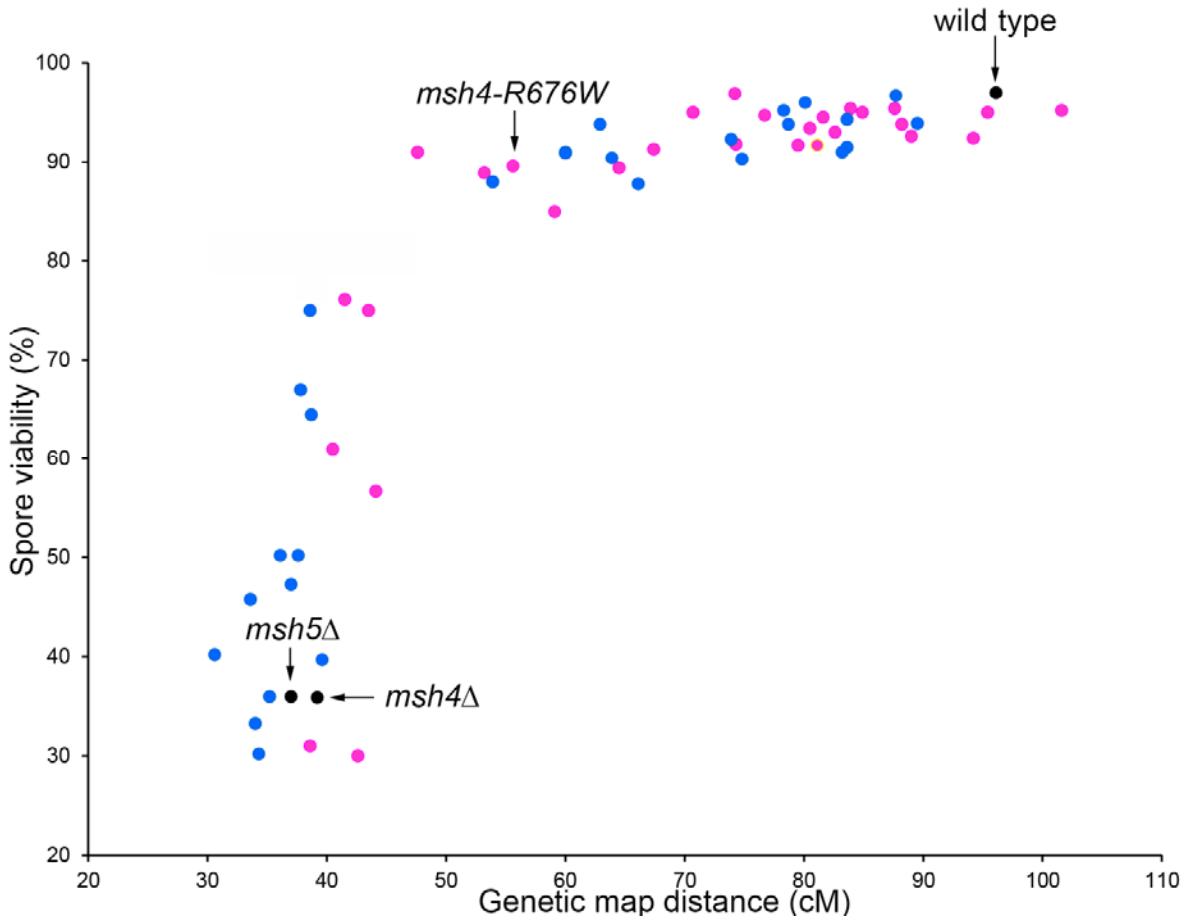

Figure S1 Spore viability and genetic map distance for specific intervals on chromosome XV plotted for 57 *msh4* (pink) *and msh5* (blue) mutants in the SK1 EAY1108/EAY1112 background. The *msh4-R676W* mutant characterized in this study is shown. Figure adapted from Nishant *et al.* 2010 with permission.

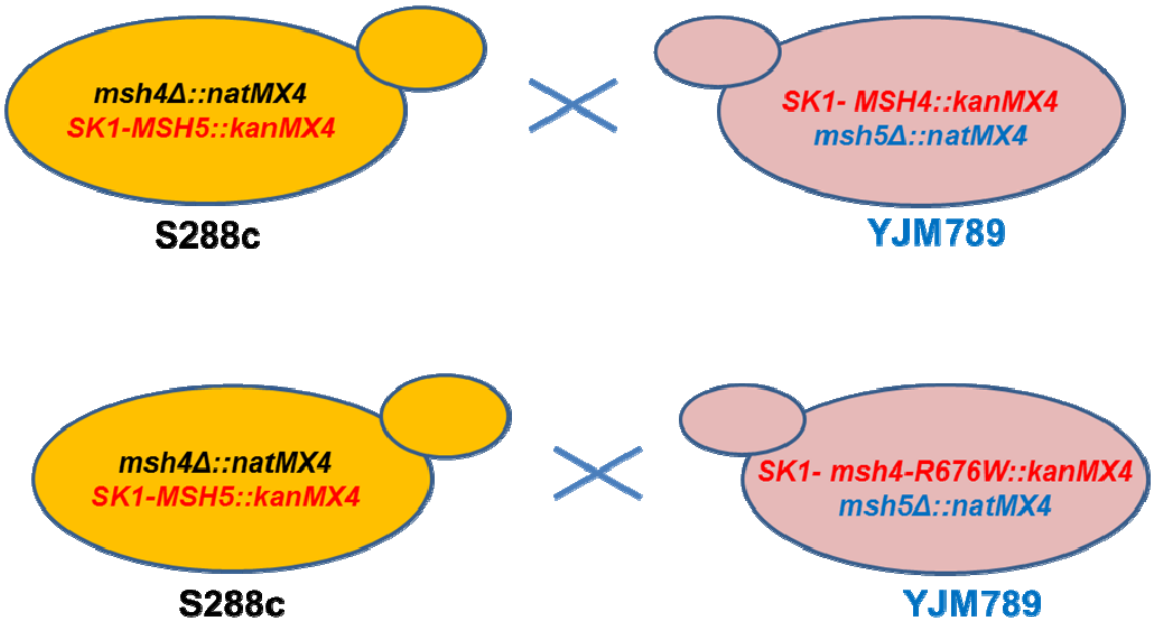

Figure S2 Construction of S288c/YJM789 hybrid with SK1 *MSH4/5* and *msh4 -R676W* mutant alleles. A single copy of the SK1 *MSH4* and *MSH5* genes and the *msh4-R676W* mutant were introduced into the *S. cerevisiae* S288c or YJM789 strains by homologous gene replacement.

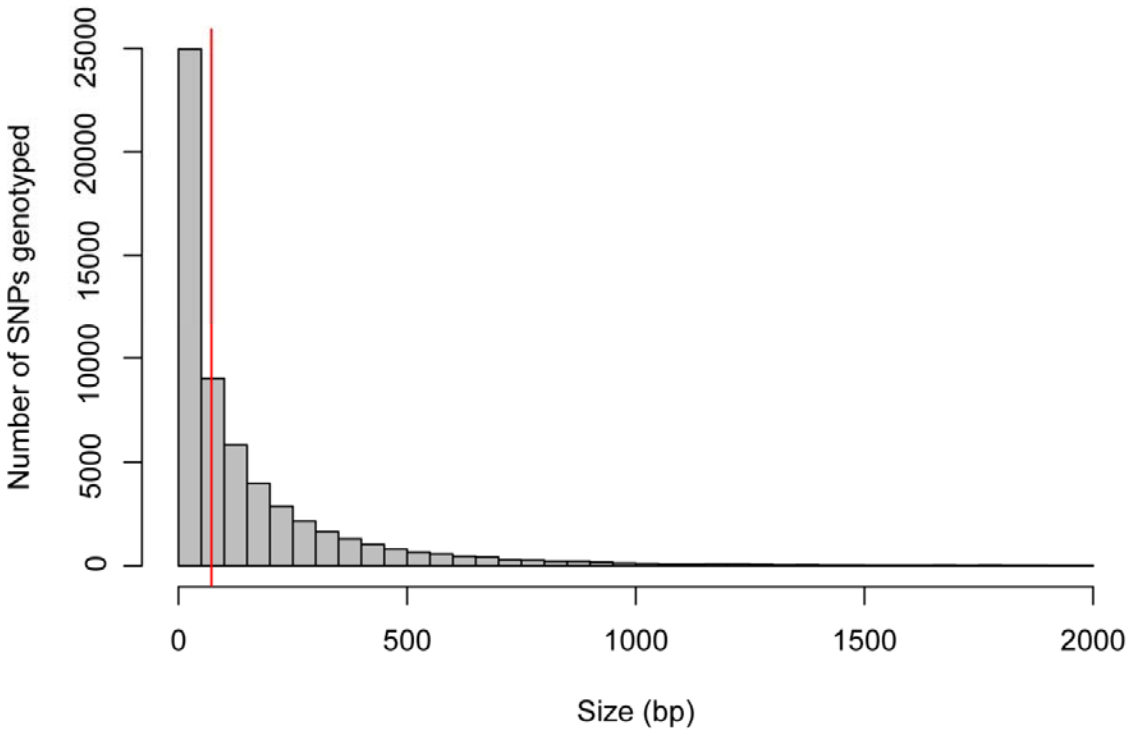

Figure S3 Inter-marker intervals in base pairs for SNPs genotyped by sequencing in the S288c/YJM789 cross. Red line indicates the median size of the interval in base pairs.

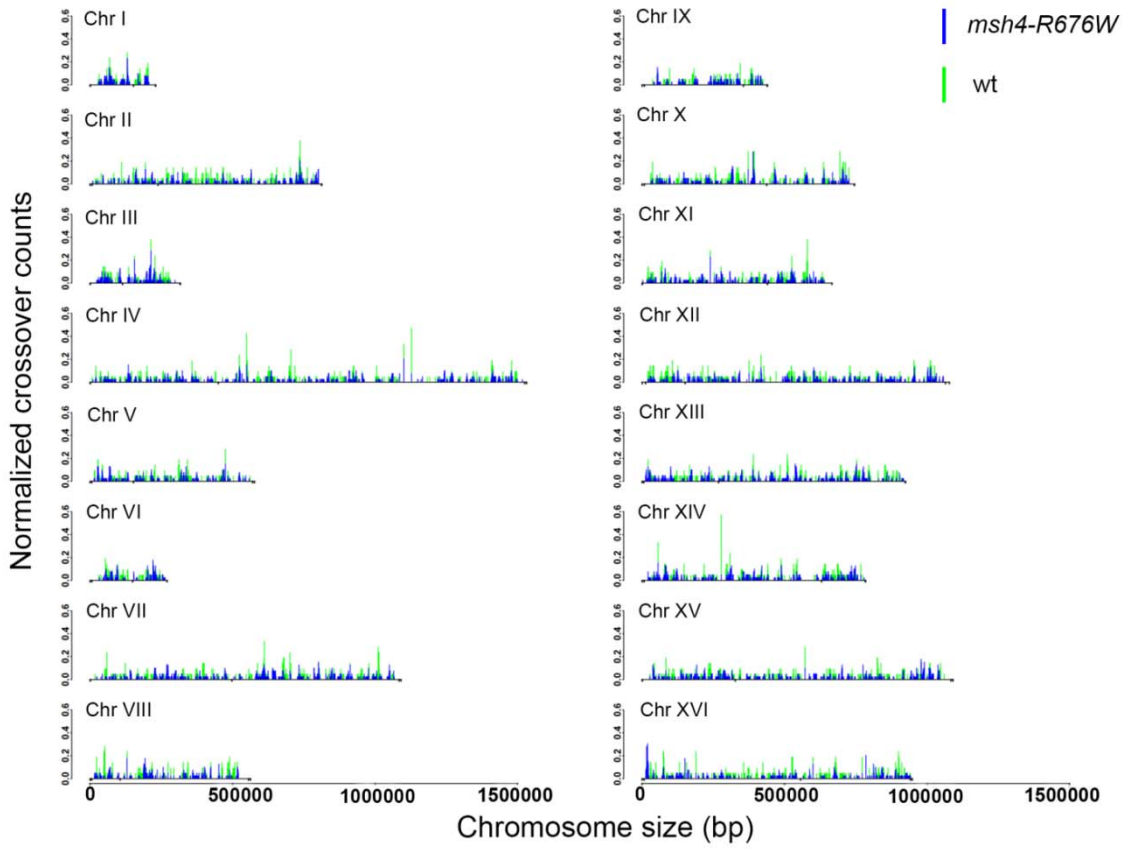

Figure S4 Genome wide crossover counts for wild type (green) and *msh4-R676W* (blue) normalized for differences in number of tetrads analyzed and varying inter-marker interval size. Actual crossover counts were divided by the number of tetrads to get normalized counts. Chromosome size is shown in base pairs.

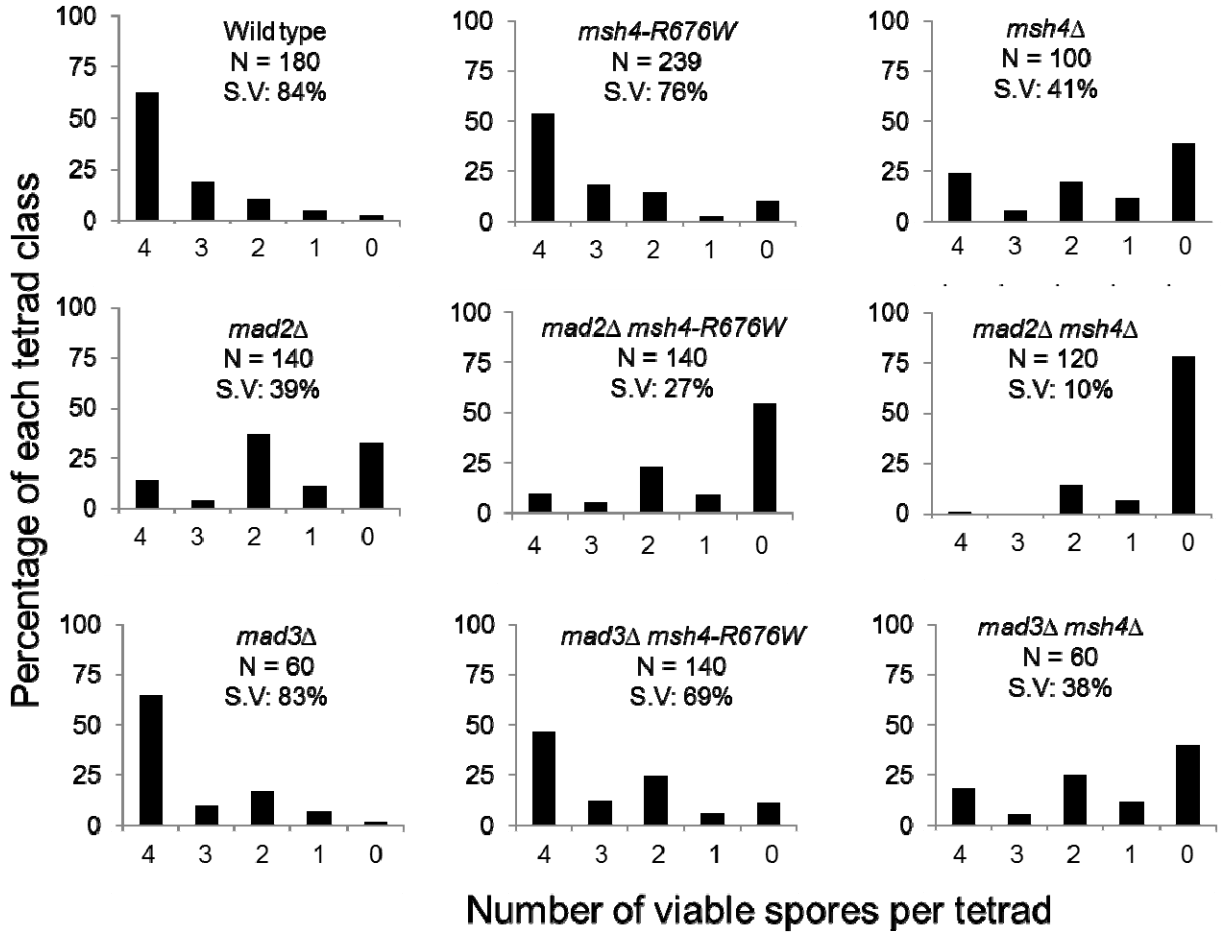

Figure S5 Spore viability analysis of wild type, *msh4-R676W*, *msh4Δ*, *mad2Δ*, *mad3Δ* single and double mutant strains. Strain background is the S288c/YJM789 hybrid. The Y axis shows the percentage of each tetrad class and the X axis indicates the number of viable spores per tetrad. N = number of tetrads dissected, S.V = percentage spore viability.

Table S1 Strains used in this study

Strain	Genotype	Source
S288c	*MATa ho lys5*	Mancera *et al.* 2008
SEM049	as S288c except *msh4Δ::natMX4*	Mancera *et al.* 2008
KTY94	as S288c except *SK1-MSH5::kanMX4, msh4Δ::natMX4*	This Study
KTY297	as S288c except *mad3Δ::kanMX4*	This Study
KTY305	as S288c except *msh4Δ:: natMX4, mad3Δ::kanMX4*	This Study
KTY301	as S288c except *SK1-MSH5::kanMX4, msh4Δ::natMX4, mad3Δ::hphMX4*	This Study
KTY317	as S288c except *mad2Δ::kanMX4*	This Study
KTY321	as S288c except *msh4Δ::natMX4, mad2Δ::kanMX4*	This Study
KTY313	as S288c except *SK1-MSH5::kanMX4, msh4Δ:: natMX4, mad2Δ::hphMX4*	This Study
YJM789	*MATα ho::hisG lys2 cyh*	Mancera *et al.* 2008
YEM002	as YJM789 except *msh4Δ::natMX4*	Mancera *et al.* 2008
KTY98	as YJM789 except *msh5Δ::natMX4, SK1-MSH4::kanMX4*	This Study
KTY108	as YJM789 except *msh5Δ::natMX4, SK1-msh4-R676W::kanMX4*	This Study
KTY295	as YJM789 except *mad3Δ::kanMX4*	This Study
KTY303	as YJM789 except *msh4Δ::natMX4, mad3Δ::kanMX4*	This Study
KTY299	as YJM789 except *msh5Δ::natMX4, SK1-msh4-R676W::kanMX4, mad3Δ::hphMX4*	This Study
KTY315	as YJM789 except *mad2Δ::kanMX4*	This Study
KTY319	as YJM789 except *msh4Δ::natMX4, mad2Δ::kanMX4*	This Study
KTY311	as YJM789 except *msh5Δ::natMX4, SK1-msh4-R676W::kanMX4, mad2Δ::hphMX4*	This Study

Tables S2-S3

Available for download as Excel files at http://www.genetics.org/lookup/suppl/doi:10.1534/genetics.114.172320/-/DC1

Table S2 Summary of sequencing statistics for spores derived from 80 wild-type and *msh4* mutant tetrads

Table S3 Count of crossovers (CO), non-crossovers (NCO) and the number of non-exchange chromosomes (NEC) in the 80 wild type and *msh4* mutant tetrads

Table S4 Average crossovers (CO) and non-crossovers (NCO) per chromosome for wild type and *msh4* mutants

Chromosome	Wild type	WT-SK1-*MSH4/5*	*msh4-R676W*	*msh4Δ*
I	2.20	0.50	1.66	0.83
II	6.40	3.75	4.45	3.61
III	3.40	3.50	2.34	2.44
IV	10.20	10.25	6.87	5.72
V	4.45	3.00	2.82	2.61
VI	2.65	1.75	1.71	1.50
VII	8.25	8.25	5.92	3.89
VIII	4.65	4.00	3.08	1.94
IX	3.00	2.75	2.03	2.11
X	6.50	6.25	3.71	3.22
XI	5.25	4.00	4.00	2.50
XII	8.65	7.25	5.55	3.67
XIII	7.25	6.75	5.05	3.89
XIV	6.40	6.75	4.63	2.78
XV	7.75	8.25	5.87	4.39
XVI	7.45	8.75	4.55	4.39
Total_CO	**94.45**	**85.75**	**64.24**	**49.5**
Chromosome	**Wild type**	**WT-SK1-*MSH4/5***	***msh4-R676W***	***msh4Δ***
I	2.00	2.50	2.55	3.44
II	3.50	4.25	3.50	5.22
III	1.30	1.00	1.95	2.61
IV	5.95	6.00	6.24	8.00
V	3.00	4.25	3.00	3.39
VI	1.70	1.75	1.71	1.39
VII	5.15	5.50	4.37	4.78
VIII	2.20	2.75	2.42	3.94
IX	2.00	3.00	2.05	3.00
X	4.05	4.00	3.16	4.78
XI	3.05	2.25	3.16	3.44
XII	4.00	5.00	5.00	5.06
XIII	5.05	4.25	4.66	5.44
XIV	3.15	2.75	3.16	4.17
XV	4.35	3.75	4.11	6.61
XVI	6.35	2.50	4.16	4.39
Total_NCO	**56.80**	**55.50**	**55.18**	**69.67**

Table S5 Chromatid interference in wild type, *msh4-R676W* and *msh4Δ*. The Chi square test shows no significant difference between expected and observed ratios of 2, 3 or 4 strand crossovers.

	Wild type	***msh4-R676W***	***msh4Δ***
Observed ratios	425:746:400	502:898:450	155:317:152
Expected ratios	392.75:785.5:392.75	462.5:925:462.5	156:312:156
P value	0.092	0.10	0.91

Table S6 Chromosome wise distribution of gene conversions observed on non-exchange chromosomes (NECs).

Minimum distance is shown for adjacent gene conversion events involving 3:1, 1:3, or 0:4, 4:0 conversion tracts only. NA (Not applicable) is shown if there are no adjacent tracts or other types of conversion are observed. N = number of events observed.

Tetrad-ID	NEC	Min. distance between consecutive gene conversions on the NEC (bp)	Gene conversion types observed (N)
WT-2	VI	NA	3:1 or 1:3 tract (1)
WT-7	IX	NA	Double CO or NCO (1)
msh4_R676W-2	III	4452.75	3:1 or 1:3 tract (8)
msh4_R676W-4	X	NA	3:1 or 1:3 tract (1)
msh4_R676W-5	VI	NA	3:1 or 1:3 tract (1)
msh4_R676W-11	I	14640.75; 71950.75	3:1 or 1:3 tract (2); 4:0 or 0:4 tract (3)
msh4_R676W-12	II	NA	4:0 or 0:4 tract (1)
msh4_R676W-21	IX	NA	No gene conversion detected
msh4_R676W-24	IX	NA	3:1 or 1:3 tract (1); 4:0 or 0:4 tract (1); Double gene conversion at chromosome end (1)
msh4_R676W-31	IX	NA	Gene conversion involving chromosome end (1)
msh4_R676W-37	I	9564.2	3:1 or 1:3 tract (1); 4:0 or 0:4 tract (3)
msh4_R676W-40	VI	65784	3:1 or 1:3 tract (3)
msh4_R676W-59	VI	179100.5	3:1 or 1:3 tract (2); Double CO or NCO (1)
msh4_R676W-64	IX	66929.5	3:1 or 1:3 tract (3); Double gene conversion involving a chromosome end (1)
msh4_R676W-65	I	88392.7	3:1 or 1:3 tract (1); 4:0 or 0:4 tract (1)
msh4_R676W-65	XI	232186.5	3:1 or 1:3 tract (2)
msh4_R676W-68	I	NA	3:1 or 1:3 tract (1); 4:0 or 0:4 tract (1)
msh4_R676W-70	IX	NA	3:1 or 1:3 tract (1); Gene conversion involving a chromosome end (1); Double CO or NCO (1)
msh4_R676W-76	VIII	NA	4:0 or 0:4 tract (1)
msh4_null-1	III	NA	3:1 or 1:3 tract (1); 4:0 or 0:4 tract (1)
msh4_null-3	I	8403.7; 65619.75	3:1 or 1:3 tract (2); 4:0 or 0:4 tract (2)
msh4_null-3	VI	2189	3:1 or 1:3 tract (3); Double CO or NCO (1)
msh4_null-4	IX	13239.75	3:1 or 1:3 tract (3)
msh4_null-9	IX	NA	3:1 or 1:3 tract (1); Double gene conversion involving a chromosome end (1)
msh4_null-9	XI	NA	Double gene conversion involving a chromosome end (1)

msh4_null-9	XII	32610	3:1 or 1:3 tract (6)
msh4_null-10	I	NA	4:0 or 0:4 tract (1)
msh4_null-10	XI	10731.75	3:1 or 1:3 tract (5); Double CO or NCO (1); 4:0 or 0:4 tract (1)
msh4_null-11	I	21688.25	3:1 or 1:3 tract (4); 4:0 or 0:4 tract (1)
msh4_null-11	VI	NA	No gene conversion detected
msh4_null-12	I	NA	3:1 or 1:3 tract (1); 4:0 or 0:4 tract (1)
msh4_null-20	I	8182.75	3:1 or 1:3 tract (2); 4:0 or 0:4 tract (1)
msh4_null-20	VI	NA	3:1 or 1:3 tract (1); 4:0 or 0:4 tract (1)
msh4_null-20	XVI	NA	3:1 or 1:3 tract (1); 4:0 or 0:4 tract (1)
msh4_null-22	V	5873.7	3:1 or 1:3 tract (3); 4:0 or 0:4 tract (1); Double gene conversion involving a chromosome end (1)
msh4_null-23	XIV	NA	3:1 or 1:3 tract (1); Double gene conversion involving a chromosome end (1)
msh4_null-24	I	1600; 123849.2	3:1 or 1:3 tract (3); 4:0 or 0:4 tract (2)
msh4_null-26	I	54269.25; 9564.25	3:1 or 1:3 tract (3); 4:0 or 0:4 tract (1)
msh4_null-26	III	118014.2	3:1 or 1:3 tract (2); Double CO or NCO (1)
msh4_null-28	I	179523.5; 75104.75	3:1 or 1:3 tract(2); 4:0 or 0:4 tract (1)
WT_SK1_MSH4_5-1	I	123753.5	3:1 or 1:3 tract (1); 4:0 or 0:4 tract (2); Double gene conversion involving a chromosome end (1)
WT_SK1_MSH4_5-3	VI	NA	3:1 or 1:3 tract (1); Double CO or NCO (1)
WT_SK1_MSH4_5-5	I	950; 78994	3:1 or 1:3 tract (7); 4:0 or 0:4 tract (3); gene conversion involving a chromosome end (1)

Out of a total of forty three non-exchange chromosomes, seven have genotype changes that can be annotated as a double non-crossover or a double crossover. These are distributed among the wild type (1); wild type with SK1-*MSH4/5* (1); *msh4-R676W* (2) and *msh4Δ* (3) tetrads. Visual inspection of the genotype changes showed that six of these regions have a maximum tract size of 3 kb which make a double crossover event unlikely. One region has tract size of 24.3 kb (*msh4Δ*) and remains ambiguous in our dataset. This ambiguity does not produce significant change in our results. For example, if we consider the region with tract size of 24.3 kb as double crossover, the average crossovers would change from 49.50 to 49.55 for *msh4Δ*. The percentage of non-exchange chromosomes for *msh4Δ* will change from 39:33:28 to 44:28:28 (one non-exchange : more than one non-exchange : no non-exchange chromosomes).

Table S7 Non-exchange events observed in the wild type and *msh4* mutants among small (I, III, VI, IX), medium (II, V, VIII, X, XI, XIV) and large (IV, VII, XII, XIII, XV, XVI) chromosomes.

	Chromosome		
Genotype	**Small**	**Medium**	**Large**
Wild type	2	0	0
msh4-R676W	13	4	0
msh4Δ	15	4	2

Table S8 Expected Poisson probabilities of observing no non-crossovers given the average non-crossovers per chromosome.

Chromosome	Probability of zero non-crossovers in wild type	Probability of zero non-crossovers in *msh4-R676W*	Probability of zero non-crossovers in *msh4Δ*
I	0.13	0.07	0.03
II	0.03	0.03	0.00
III	0.27	0.14	0.07
IV	0.00	0.00	0.00
V	0.05	0.05	0.03
VI	0.18	0.18	0.25
VII	0.00	0.01	0.00
VIII	0.11	0.09	0.02
IX	0.13	0.13	0.05
X	0.02	0.04	0.00
XI	0.05	0.04	0.03
XII	0.02	0.00	0.00
XIII	0.00	0.00	0.00
XIV	0.04	0.04	0.01
XV	0.01	0.02	0.00
XVI	0.00	0.01	0.01
Expected frequency of chromosomes with zero non-crossovers per cell	1.07	0.89	0.55
Observed frequency of chromosomes with zero non-crossovers per cell	1.2	1.1	0.77

The expected Poisson probability of observing zero non-crossovers on a chromosome was calculated using the mean number of non-crossovers observed for that particular chromosome (λ) from experimental data and the formula: $P(k) = \lambda^k e^{-\lambda} / k!$. For example, since the mean number of non-crossovers on chromosome III is 1.3, the expected probability of zero non-crossovers (k=0), is $P(k=0 \mid \text{mean non-crossover} = 1.3) = e^{-1.3} = 0.27$.

Table S9 Non-exchange chromosomes (E0s) show reduced gene conversion events compared to exchange chromosomes (Non E0s). Non-exchange and exchange chromosomes were analysed for the number of gene conversion events not associated with crossovers across the three genotypes (Wild type, *msh4-R676W* and *msh4Δ*).

	E0	Non E0
Expected total number of gene conversion events	137.7	4880.3
Observed total number of gene conversion events	125	4893

The total observed count of gene conversions not associated with crossovers in the non-exchange chromosomes (E0s) is lower than expected. We tested whether the deviation between observed and expected gene conversions counts in the non-exchange chromosome is significant by using a Poisson regression that adjusts for potential over dispersion (general linearized model with quasi-Poisson). In the full (saturated) model, the expected gene conversion counts are dependent on the chromosome, the genetic background and whether the chromosome has no crossovers on it. So the expected gene conversion counts for both E0 and non-E0 would be the observed counts under the full model. In the reduced model, the expected gene conversion counts are only dependent on the chromosome and the genetic background and would be as shown in the table. Therefore in the reduced model, the fitted value for each chromosome is the average gene conversion counts for each chromosome in the three genetic backgrounds. The expected total gene conversions were obtained by summing up the gene conversion counts under the reduced model across all three genotypes for the non-exchange chromosomes. A similar procedure was followed to calculate the expected gene conversion counts for the exchange chromosomes. Next we estimated the likelihood of the full model and the reduced model, given the observed data. The difference in likelihood between the two models allows us to estimate the significance of observing such a result, assuming an F distribution. Comparing the full model with the reduced model, we estimated that chromosomes with no crossovers (E0s) receive 75% of the gene conversions compared to chromosomes with a crossover (p value = 0.02).

File S1

Supporting data

Segregation plots of SNPs from the S288c/YJM789 hybrid for wild type, *msh4-R676W*, *msh4Δ* and wild type with SK1 *MSH4/5* alleles

File S1 is available for download as a zip file at

http://www.genetics.org/lookup/suppl/doi:10.1534/genetics.114.172320/-/DC1

File S2

Crossover and non-crossover distributions along centromeres and telomeres in wild type, *msh4-R676W* and *msh4Δ*

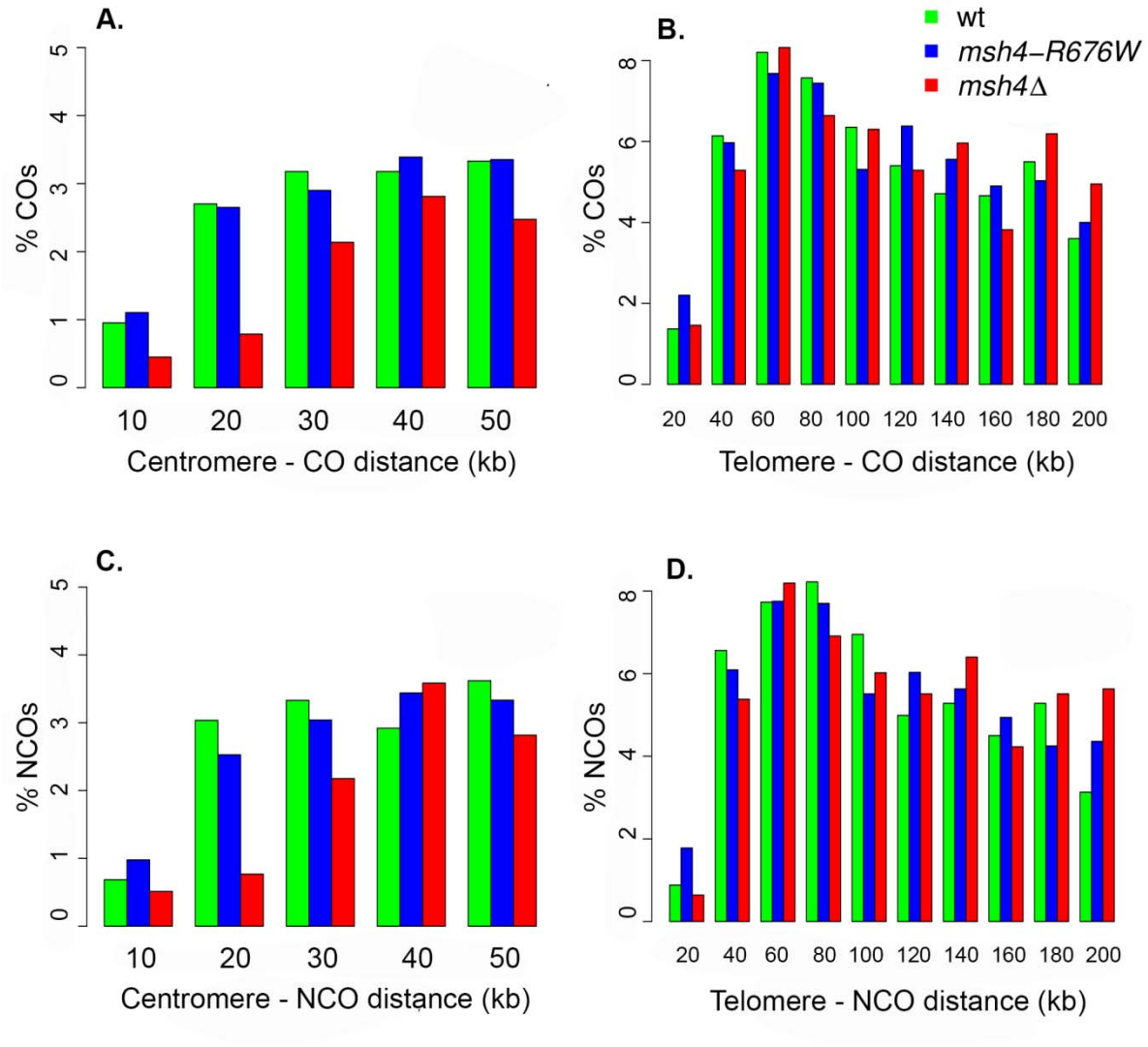

Figure 1 Crossover and non-crossover distributions near centromeres (Panels A and C) and telomeres (Panels B and D) in wild type, *msh4-R676W* and *msh4Δ*. Crossover and non-crossover events are shown as a percentage of the total number of events.

To analyze if crossover placement is affected in the *msh4-R676W* hypomorph we examined the distribution of crossovers near centromere and telomere regions in wild type and *msh4* mutants (**Figure 1**). Wild-type strain showed reduction in both crossovers (2.8 fold) and non-crossovers (4.4 fold) within 10 kb of centromeres as observed by Chen *et al.* 2008 (**Figure 1A, C**). Similar reductions in crossover (2.6 fold) and non-crossover (3.1 fold) levels were observed in the *msh4-R676W* mutant. *msh4Δ* mutants also showed suppression in crossover (2.6 fold) and non-crossover (3.1 fold) levels that extended for a longer distance from the centromeres (up to 30 kb). Crossovers in wild type were suppressed by 4.5 fold

within 20 kb of telomeres as observed previously in Chen *et al.* 2008 (**Figure 1B**). The *msh4-R676W* and *msh4Δ* mutants showed a 2.7 and 3.6 fold suppression, compared to surrounding genomic regions. Non-crossovers were similarly reduced in wild type (7.4 fold), *msh4Δ* (8.45 fold) and *msh4-R676W* (3.4 fold) strains within ~20 kb of telomeres (**Figure 1D**). For wild type Chen *et al.* 2008 observed no significant reduction in non-crossovers close to telomeres. This difference may be due to fewer numbers of non-crossovers per tetrad (~18) detected in Chen *et al.* 2008 due to lower resolution of markers.

Supplementary reference

Chen, S.Y., T. Tsubouchi, B. Rockmill, J.S. Sandler, D.R. Richards *et al.*, 2008 Global analysis of the meiotic crossover landscape. Dev Cell 15: 401-415.

File S3

Gene conversion in wild type and *msh4* mutants

The majority (> 97.5%) of markers genotyped in the wild type and *msh4* mutants showed 2:2 segregation (**Table 1**). These values are in agreement with previous estimates of marker segregation frequencies in wild type and crossover mutants (Chen *et al.* 2008; Mancera *et al.* 2008). The median size of conversion tracts associated with crossovers and non-crossovers is shown in **Table 2**. The mid-point between markers that show switching from one genotype to the other were used for measuring gene conversion tract lengths. The median gene conversion tract lengths associated with crossovers (2.2 kb) were longer than the non-crossover gene conversion tract lengths (1.1 kb) for wild type consistent with previous observations (Jeffreys and May 2004; Terasawa *et al*. 2007; Mancera *et al*. 2008; Chen *et al*. 2008; Oke *et al.* 2014). These differences are statistically significant (Wilcoxon rank-sum test, $P = 2.2 \times 10^{-16}$). Our estimates for the wild-type tract lengths are 244 bp longer for crossover associated tracts and 659 bp shorter for non-crossover tracts compared to the Mancera *et al.* 2008 study. The *msh4-R676W* and *msh4Δ* mutants also showed increased median conversion tract lengths for crossovers compared to non-crossovers which were statistically significant (**Table 2, Figure 2**). These observation's suggest crossover associated gene conversion tracts are longer than non-crossover tracts even in crossover mutants as observed previously for *msh4Δ* (Mancera *et al*. 2008; Chen *et al.* 2008; Oke *et al.* 2014). Previously Mancera *et al.* 2008 also observed that crossover associated tract lengths for *msh4Δ* mutants are 479 bp longer than wild type and the non-crossover associated tract lengths are 338 bp shorter than wild type. We observed *msh4Δ* crossover associated tracts were longer by 709 bp (Wilcoxon rank-sum test, $P = 5.33 \times 10^{-9}$) compared to wild type similar to the Mancera *et al.* 2008 study. Crossover associated conversion tracts were not significantly different from wild type in *msh4-R676W* (84 bp increase, Wilcoxon rank-sum test, $P = 0.8487$). Non-crossover associated tracts were also significantly longer in *msh4Δ* (494 bp increase, Wilcoxon rank-sum test, $P = 2.94 \times 10^{-16}$) and the *msh4-R676W* (578 bp increase, Wilcoxon rank-sum test, $P = 2.2 \times 10^{-16}$) mutant compared to wild type. Similar increase in *msh4Δ* crossover and non-crossover tract length compared to wild type has been observed by Chen *et al.* 2008. However a recent study by Oke *et al.* 2014 shows no significant difference in non-crossover tract lengths between *msh4Δ* and wild type. The proportion of conversion tracts that show 4:0 segregation of markers was approximately two fold higher in *msh4-R676W* and *msh4Δ* mutants compared to wild type (*Z* test, $P < 0.001$, **Table 3**). Two fold increase in conversion tracts extending to chromosome ends was also observed in *msh4-R676W and msh4Δ* mutants relative to wild type (*Z* test, $P < 0.001$). Complex conversion tracts involving multiple genotype changes on the chromatids involved were observed at similar frequencies (*Z* test, $P > 0.05$) in wild type (1.98%), *msh4-R676W* (2.93%) and *msh4Δ* (2.65%) mutants. The average count/tetrad of all gene conversion tracts not associated with crossovers was 60.3, 62.7 and 79.4 for wild type, *msh4-R676W* and *msh4Δ* respectively and statistically significant between *msh4Δ* and wild type (*t* test, p = 0.028).

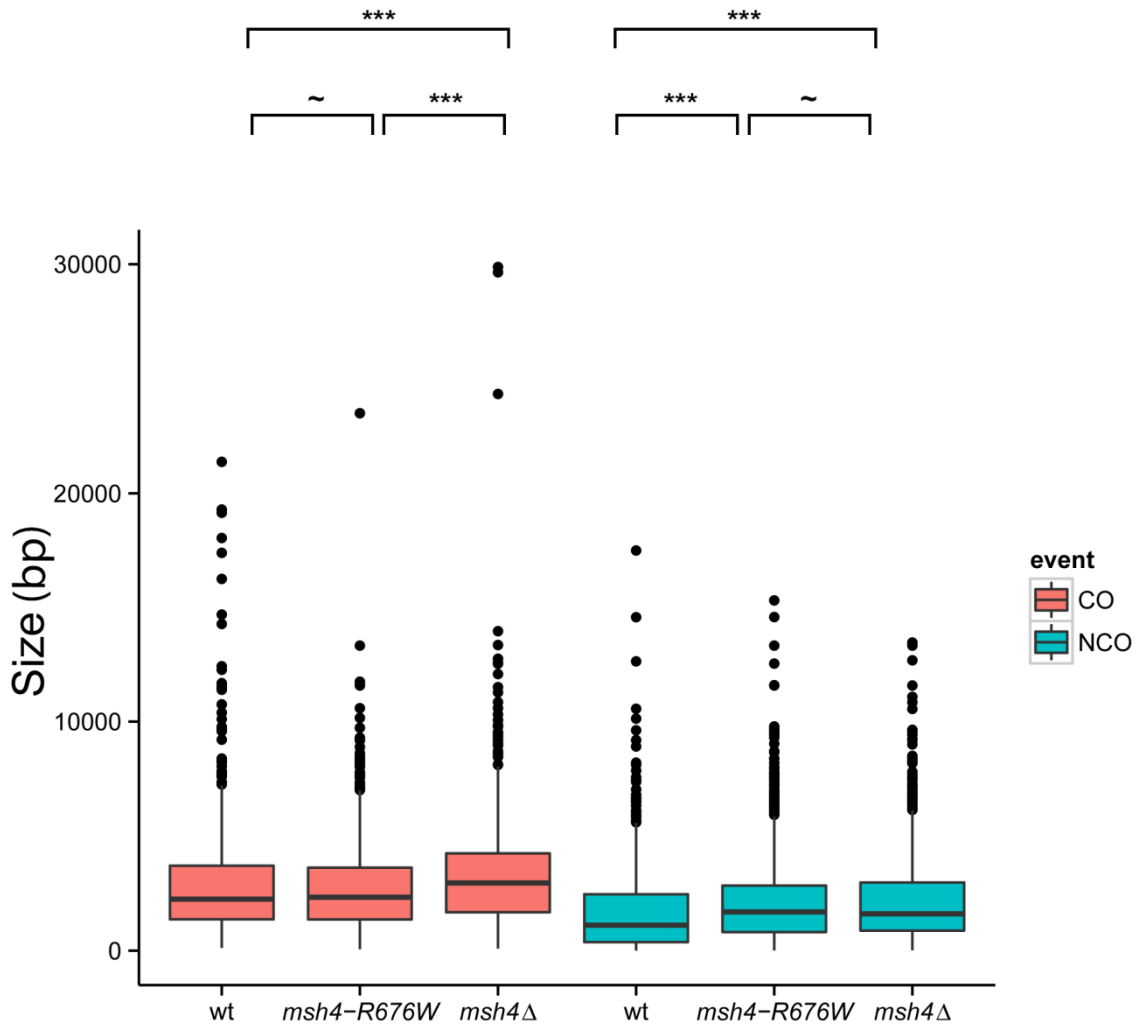

Figure 2 Gene conversion tract size distributions associated with crossovers and non-crossovers for wild type, *msh4-R676W* and *msh4Δ*. An asterisk (***) indicates statistically significant difference between the two groups ($P < 0.001$), whereas a tilde (~) indicates no significant difference ($P > 0.001$).

Table 1 Marker segregation frequency. The percentage of SNP markers showing 2:2, 3:1, 1:3, 4:0 and 0:4 segregation (S288c:YJM789) is shown.

Strain	2:2	3:1	1:3	4:0	0:4
Wild type	97.96	0.93	1.03	0.03	0.03
msh4-R676W	98.05	0.94	0.92	0.04	0.03
msh4Δ	97.50	1.01	1.20	0.04	0.24

Table 2 Gene conversion tract lengths in wild type and *msh4* mutants. Median gene conversion tract lengths are shown. *P* values estimate if the difference between median crossover (CO) and non-crossover (NCO) gene conversion length is statistically significant.

Genotype	NCO tract length in bp (max. in kb)	CO tract length in bp (max. in kb)	Wilcoxon rank-sum test, *P* value
Wild type	1116 (17.47 kb)	2250 (21.39 kb)	2.2×10^{-16}
msh4-R676W	1694 (15.29 kb)	2334 (23.5 kb)	2.2×10^{-16}
msh4Δ	1610 (13.4 kb)	2959 (29.88 kb)	2.2×10^{-16}

Table 3 Percentage of complex gene conversion events, conversion tracts extending to the chromosome end and 4:0 tracts. The *Z* test shows if the percentage of these events in *msh4* mutants are statistically different from wild type.

Genotype	Complex conversion tracts	Tract extending to chromosome end	4:0 tracts
Wild type	1.98	1.82	2.00
msh4-R676W	2.93	3.93	3.75
	(P = 0.116)	(P = 2.4 x 10^{-4})	(P < 0.001)
msh4Δ	2.65	4.02	4.52
	(P = 0.337)	(P = 3.6 x 10^{-4})	(P < 0.001)

Supplementary references

Chen, S.Y., T. Tsubouchi, B. Rockmill, J.S. Sandler, D.R. Richards *et al.*, 2008 Global analysis of the meiotic crossover landscape. Dev Cell 15: 401-415.

Jeffreys, A.J., and C.A. May, 2004 Intense and highly localized gene conversion activity in human meiotic crossover hot spots. Nat Genet 36: 151-156.

Mancera, E., R. Bourgon, A. Brozzi, W. Huber, and L.M. Steinmetz, 2008 High-resolution mapping of meiotic crossovers and non-crossovers in yeast. Nature 454: 479-485.

Oke, A., C.M. Anderson, P.Yam, and J.C. Fung, 2014 Controlling meiotic recombination repair-specifying the roles of ZMMs, Sgs1 and Mus81/Mms4 in crossover formation. PLoS Genet 10: e1004690.

Terasawa, M., H. Ogawa, Y. Tsukamoto, M. Shinohara, K. Shirahige *et al.*, 2007 Meiotic recombination-related DNA synthesis and its implications for cross-over and non-cross-over recombinant formation. Proc Natl Acad Sci U S A 104: 5965-5970.

File S4

Modeling the role of interference in ensuring the obligate crossover

If we assume the crossover distribution on each chromosome follows a Poisson distribution with no interference, then the probability of observing no chromosomes with 0 crossovers for chr *i* with mean number of crossovers λ_i is:

$1 - P(X_i=0) = 1 - \exp(-\lambda_i)$

Then to observe no chromosomes with 0 crossovers (non-exchange chromosomes) on all 16 chromosomes, the probability is:

$(1 - \exp(-\lambda_{chr01}))* (1 - \exp(-\lambda_{chr02})) .. (1 - \exp(-\lambda_{chr16}))$

which can be simplified as:

$\text{Exp} (\Sigma_{i=chr01..chr16} \log(1 - \exp(-\lambda_i)))$

If the mean crossovers per chromosome change uniformly by a factor of t, then the probability of observing no non-exchange chromosomes in all 16 chromosomes is:

$\text{Exp}(\Sigma_{i=chr01..chr16} \log(1 - \exp(- t * \lambda_i)))$

As the average number of crossovers gets larger ($t \rightarrow \infty$), the probability of observing no E0 chromosomes across all 16 chromosomes approaches 1. Using the data for average number of crossovers per chromosome in wild type, *msh4-R676W* and *msh4Δ*, the average total crossover number (t*sum(mean crossover per chromosome)) , was plotted against the probability (black dots) of observing no E0s per cell (**Figure 3**). The same plot (red dots) was also generated for wild type, *msh4-R676W* and *msh4Δ* by modeling crossovers with interference (as described below). The difference between the two plots (red and black) is negligible for *msh4Δ* and becomes increasingly significant with the progressive gain in interference for *msh4-R676W* and wild type. These observations suggest an important role for interference in ensuring the obligate crossover given an average number of crossovers per meiosis. For wild type, if the crossovers followed a Poisson distribution (no interference), an average of 200 crossovers per meiosis will be required for seeing no E0s (Probability ≥ 0.98).

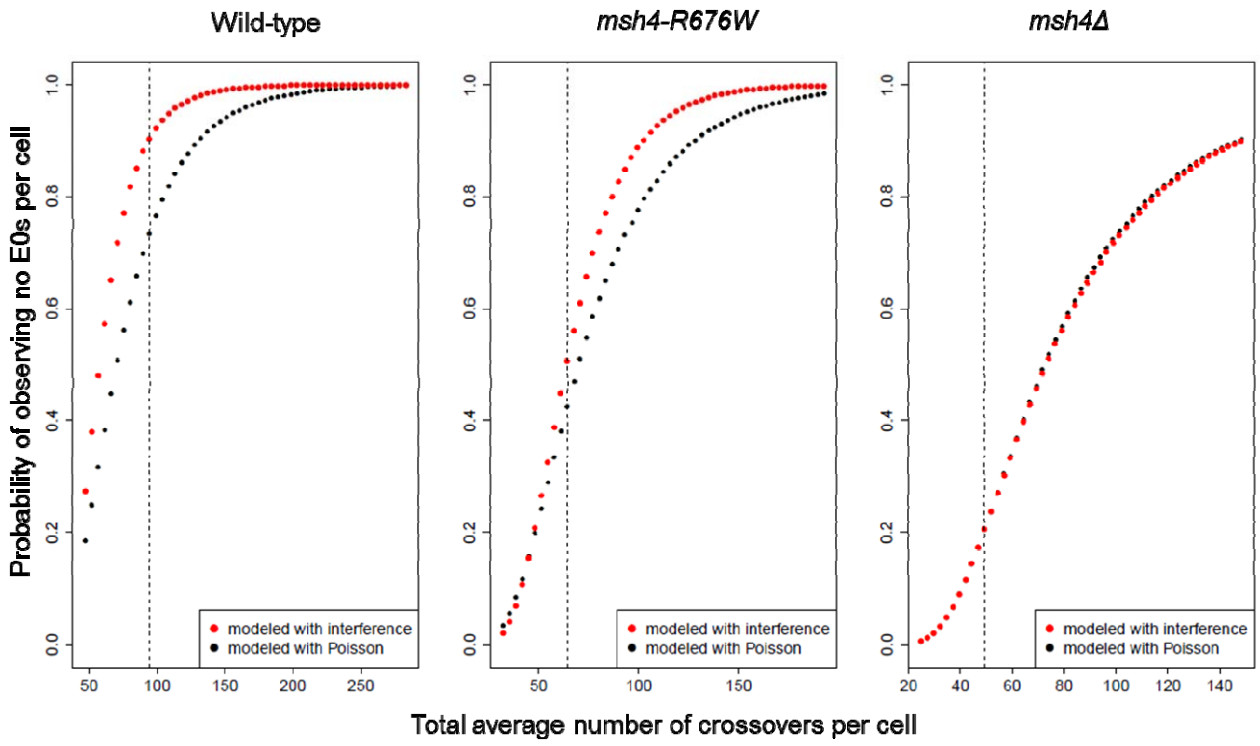

Figure 3 Plot of probability of observing no E0s for a cell for each of the genotypes, given an average number of total crossovers per cell. For the Poisson model (black dots), the crossover on each chromosome is assumed to follow a Poisson distribution with the average crossovers for each chromosome obtained from the observed crossover counts (across wild type, *msh4-R676W* and *msh4Δ*). For the model with interference (red dots), the Conway-Maxwell-Poisson distribution was used (with the dispersion parameter estimated separately for each chromosome) to estimate the probability of observing no E0s in one cell (see modeling crossovers with interference below). The dotted line in each panel indicates the probabilities for observing no E0s for the experimentally observed average number of crossovers per cell (94 in wild type, 64 in *msh4-R676W* and 49.5 in *msh4Δ*) in the presence and absence of interference.

Modeling crossovers with interference

Compared to the expectation based on the Poisson distribution, the experimentally observed crossover count data was under dispersed (**Figure 4**). In general we observe a lack of crossover counts at the extreme values in experimental data due to interference and the process of formation of an obligate crossover on every homolog pair. To estimate the probability of seeing a chromosome with no crossover in the presence of interference, we used a Conway-Maxwell-Poisson distribution, which is a modified Poisson model that takes into account this under dispersion due to interference.

The probability of observing k crossovers for chr *i* with mean number of crossovers λ_i is:

$P(X_i=k) = y^k / ((k!)^\nu * Z(y,\nu))$,

where ν_i is the dispersion parameter and $Z(y,\nu)$ is the normalizing constant. Values of ν that are less than 1 indicates over dispersion where $\nu > 1$ indicate under dispersion. (For details see Shmueli *et al.* 2005).

y_i and ν_i are estimated for each chromosome from the observed distribution of crossover counts by maximum likelihood using the R package compoisson, and the probability of observing no non-exchange chromosomes in all 16 chromosomes is estimated using the fitted values of y_i and ν_i.

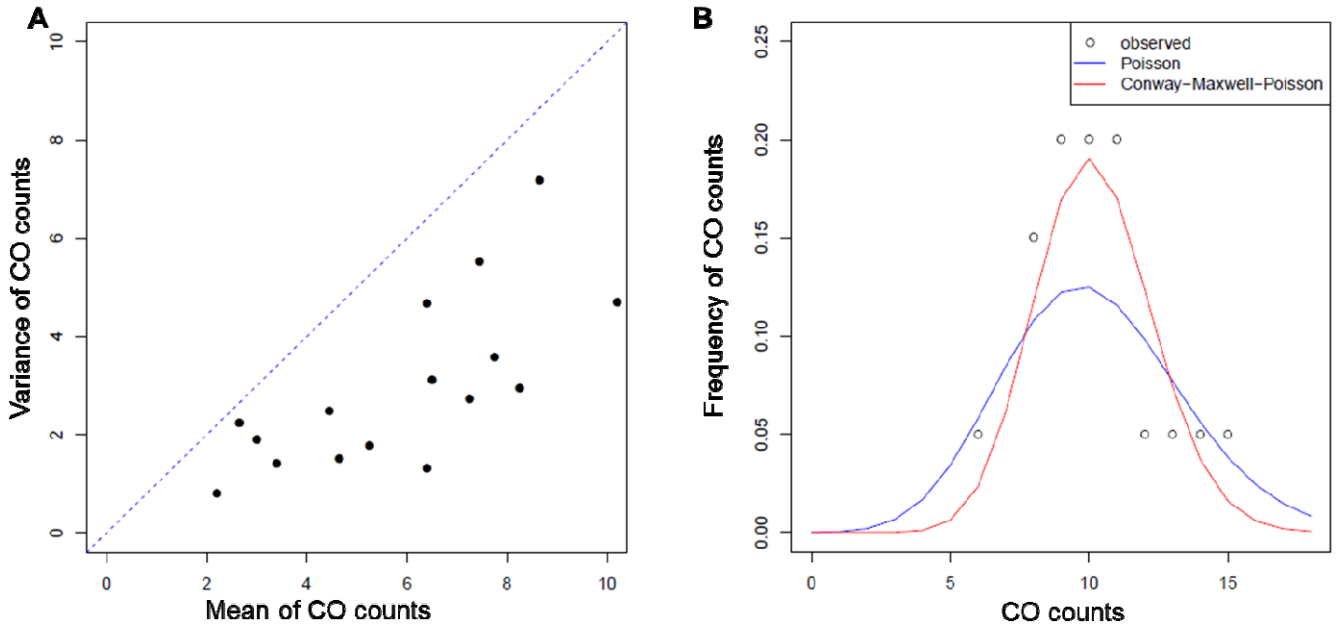

Figure 4 A) Plot of variance of crossover counts versus mean crossover counts. The variance of crossovers counts for each chromosome is plotted as against the mean of crossover counts. Under a Poisson distribution, the variance of the counts would be the mean, denoted by the blue dotted line. The observed variance is consistently less than the expected Poisson variance, indicating the under dispersion in crossover counts. **B) Distribution of crossover counts for chromosome IV modeled in the absence of interference (Poisson) and correcting for interference (Conway-Maxwell-Poisson).** More dispersion is observed under a Poisson distribution.

Supplementary literature

Shmueli, G., T.P. Minka, J.B. Kadane, S. Borle, and P. Boatwright 2005 A useful distribution for fitting discrete data: revival of the Conway-Maxwell-Poisson distribution. Applied Statistics 54: 127-142.